





Cite this: DOI: 10.1039/c8ee01373j

Recent developments and insights into the understanding of Na metal anodes for Na-metal batteries

Yang Zhao,  Keegan R. Adair and Xueliang Sun *

Rechargeable Na-based battery systems, including Na-ion batteries, room temperature Na–S, Na–O₂, Na–CO₂, and all-solid-state Na metal batteries, have attracted significant attention due to the high energy density, abundance, low cost, and suitable redox potential of Na metal. However, the Na metal anode faces several challenges, including: (1) the formation of Na dendrites and short circuiting; (2) low Coulombic efficiency (CE) and poor cycling performance; and (3) an infinite volume change due to its hostless nature. Furthermore, the issues associated with Na metal anodes have also been noticed in practical Na metal batteries (NMBs). In recent years, the importance of the Na metal anode has been highlighted and many studies have provided potential solutions to address the issues of its use. This review article focuses on the recent developments of Na metal anodes, including insight into the fundamental understanding of its electrochemical processes, novel characterization methods, approaches for protecting the anode and future perspectives. Our review will accelerate further improvement in the characterization and application of Na metal anodes for next-generation NMB systems.

Received 10th May 2018,
Accepted 16th July 2018

DOI: 10.1039/c8ee01373j

rsc.li/ees

Broader context

The global energy shortage related to the consumption of fossil fuels has become a major concern, leading to a demand for alternative clean energy sources. Energy storage systems with high energy density and low cost are characteristics that are highly sought after. Rechargeable Na metal batteries, using metallic Na as the anode electrode, have attracted increasing attention due to their high energy density and abundance, low cost, and suitable redox potential of Na metal. However, there are serious challenges including Na dendrite formation and the corresponding safety concern, unstable interface between electrolyte and Na metal, low Coulombic efficiency, poor cycling stability, and infinite volume change. In this review, we give a comprehensive summary of the recent developments and understandings of Na metal anode for room temperature Na metal batteries. Deep insights, including the fundamental understand and challenges of Na metal anode, the comparison between Li and Na metal anode, novel characterization methods, various strategies for stabilization of Na, and different types of Na metal batteries, have been discussed in detail. Future directions and prospects for long life time and high-performance Na metal anodes are also proposed.

1. Introduction

1.1 Na-ion and Na-metal batteries

Over the past decades, the global energy shortage related to the consumption of fossil fuels has become a major concern leading to the demand for alternative clean energy sources. Energy conversion techniques such as wind and solar-generated electricity have been thoroughly explored to maximize energy generation. However, they usually provide intermittent energy, which requires highly effective energy storage systems. Rechargeable Li-ion batteries (LIBs) have been developed and are one of the most promising energy storage systems, particularly for portable electronic devices such as laptops,

mobile phones, medical microelectronic devices, and even electrical vehicles (EVs).^{1,2} They have many outstanding features, including high energy density, no memory effect, low maintenance, and little self-discharge.^{3–6} The demanding requirements of portable electronic devices has stretched the limits of LIBs, which are currently the predominant choice for energy storage. Moreover, the global EVs market is quickly growing, in which the sales of EVs has increased by fifteen times in the past five years.⁷ However, the enormous demands for LIBs is dependent on the availability of Li resources, and Li is not regarded as an abundant element in the Earth's crust. Unfortunately, the cost of Li-containing materials has also rapidly increased in the past years, resulting in increased prices for LIBs.^{8,9}

Because of the high abundance, low cost, and suitable redox potential of Na metal ($E_{\text{Na}^+/\text{Na}} = -2.71$ V vs. standard hydrogen

Department of Mechanical and Materials Engineering, University of Western Ontario, London, Ontario, N6A 5B9, Canada. E-mail: xsun@eng.uwo.ca

electrode), rechargeable Na batteries are considered to be ideal alternatives to LIBs.¹⁰ In the early stages of development, many studies focused on high temperature rechargeable Na batteries such as Na-S and Na/NiCl₂ systems.¹¹ These batteries have been commercialized as large scale energy storage systems, however, the high operating temperature of 300 °C and corrosion issues limit their further application. Following a similar mechanism to LIBs, Na ion batteries (NIBs) have been developed consisting of Na insertion-type electrode materials, in which the Na⁺ is transported through the liquid electrolyte.¹² Different materials have been investigated as cathode materials for NIBs, including layered transition metal oxides (NaFeO₂, O3-Type Na[Fe_{1/2}Mn_{1/2}]O₂, P3-type Na_xCoO₂, *et al.*), polyanionic compounds (NaFePO₄, Na₂FeP₂O₇, Na₃V₂(PO₄)₃, *etc.*) and other miscellaneous Na insertion materials.^{13–15} As for the choice of anode materials, the typical graphite found in LIBs cannot be used due to it being less electrochemically active in Na⁺ systems. In 2000, Dahn's group firstly reported the electrochemical reversibility of Na⁺ insertion into hard carbon at room temperature.

The hard carbon displayed a capacity of 300 mA h g⁻¹, which is superior to that of graphite in Na batteries.^{13,16} To further improve the capacities of the anode, different alloy materials (such as Sn, Bi, Sb, and P) have been developed using various approaches such as nanostructured or composite materials.^{17–21} Some excellent reviews have summarized the development and understanding of both cathode and anode materials for NIBs in detail.^{13,18,22–25} However, the energy densities of NIBs using current cathode and anode materials are still insufficient and lower than that of commercial LIBs.²³ In this case, the development of Na-metal batteries (NMBs) with high energy density and low cost are needed to meet the requirements for large scale energy storage systems.

One of the most promising categories of NMBs is the Na-S battery system, which offers a high theoretical capacity and high energy density of ~1672 mA h g⁻¹ and 1230 W h kg⁻¹ based on the final discharge products of Na₂S.²⁶ As mentioned above, high-temperature Na-S batteries operating at 300 °C have been previously developed. The high operation temperature will decrease the energy efficiency of the device and may also cause corrosion in the system.²⁶ Researchers are beginning to explore safer and more stable room temperature (RT) Na-S batteries with high energy density. However, the RT Na-S batteries suffer from low electrochemical utilization of the sulfur active material, capacity fading, polysulfide dissolution, and short life times.^{26,27} Efforts have been mainly focused on the design of cathode materials (such as sulfurized polyacrylonitrile, sulfur-carbonaceous composites and sodium polysulfide/sulfide composites) and modification of electrolyte and separators, which have been discussed in detail in a recent review.²⁷

Another attractive NMB system is the Na-O₂ (or Na-air) battery, which also presents a high energy density of 1602 and 1105 W h kg⁻¹ based on the discharge products of Na₂O₂



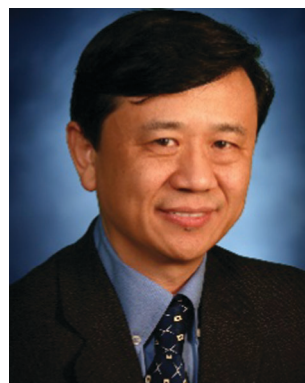
Yang Zhao

Yang Zhao is currently a PhD candidate in Prof. Xueliang (Andy) Sun's Group at the University of Western Ontario, Canada. He received his BS degree and MS degree from Northwestern Polytechnical University (Xi'an, China) in 2011 and 2014, respectively. His current research interests focus on atomic layer deposition/molecular layer deposition in the application of lithium/sodium ion batteries and all-solid-state batteries.



Keegan R. Adair

Keegan Adair received his BSc in chemistry from the University of British Columbia in 2016. He is currently a PhD candidate in Prof. Xueliang (Andy) Sun's Nanomaterials and Energy Group at the University of Western Ontario, Canada. Keegan has previous experience in the battery industry through internships at companies including E-One Moli Energy and General Motors R&D. His research interests include the design of nanomaterials for lithium metal batteries and nanoscale interfacial coatings for battery applications.



Xueliang Sun

Prof. Xueliang (Andy) Sun is a Canada Research Chair in Development of Nanomaterials for Clean Energy, Fellow of the Royal Society of Canada and Canadian Academy of Engineering and Full Professor at the University of Western Ontario, Canada. Dr Sun received his PhD in materials chemistry in 1999 from the University of Manchester, UK, which he followed up by working as a postdoctoral fellow at the University of British Columbia, Canada and as a Research Associate at L'Institut National de la Recherche Scientifique (INRS), Canada. His current research interests are focused on advanced materials for electrochemical energy storage and conversion, including electrocatalysis in fuel cells and electrodes in lithium-ion batteries and metal-air batteries.

and NaO₂, respectively.^{28–31} Compared with Li–O₂ batteries, the Na–O₂ system has the advantage of superior energy efficiency due to a lower charging over-potential in the formation of Na₂O₂ discharge products.^{32–36} In 2011, Peled *et al.* reported the first example of Na–O₂ batteries working at a temperature above the melting point of Na, followed by Sun *et al.* who demonstrated the first rechargeable Na–O₂ batteries at room temperature in 2012.^{37,137} Since then, these battery systems have achieved growing interests, however, there are still several challenges that need to be addressed in order to obtain long life Na–O₂ batteries. Our previous review gave a comprehensive summary on the challenges in the Na–O₂ battery system, including the control of discharge products, formation of parasitic products, instability of electrolyte, contamination of Na anode and poor cycling life.³⁷

Beyond liquid-based NMBs, solid-state Na metal batteries (SSNMBs) have recently become a very hot topic due to their improved safety, high-energy densities, and high-power densities achieved by replacing the organic liquid electrolyte with solid-state electrolytes (SSEs).^{38,39} Different Na-based SSEs, including solid polymer electrolytes, oxide-based ceramic electrolytes, sulfide-based electrolytes and hybrid solid electrolytes have been developed with enhanced ionic conductivity at RT with good chemical/electrochemical stability.^{38,40–44} Meanwhile, carbon materials or alloys (such as Na–Sn alloy) have also been used as anode materials in conjunction with SSEs.^{45,46}

1.2 Na metal anodes

Several types of NMBs, including RT Na–S batteries, Na–O₂ batteries and SSNMBs, are capable of delivering high theoretical energy densities and have attracted increasing attention as promising alternatives to LIBs for large scale energy storage applications. There is a common point for all these NMBs, in which Na metal is used as the anode. Compared with other anode candidates, Na metal is the ultimate choice among them due to its high theoretical capacity (1166 mA h g^{−1}) and low electrochemical potential. All theoretical specific energy densities of RT Na–S, Na–O₂ and SSNB systems are calculated by using Na metal as the anode.

Similar to the Li metal anode, Na metal also faces several crucial problems and challenges during electrochemical cycling.⁴⁷ The major issues of the Na metal anode can be summarized as: (1) Na dendrite formation and short circuits. In a typical cycling process, Na⁺ will come into contact with electrons from an external circuit during charging and then electrochemically deposit on the surface of Na metal.^{48,49} Similar to the electro-deposition behaviors of Li⁺ and Zn²⁺, dendritic structures can form on the surface of the Na metal or substrate, which is affected by various factors including current density, anion mobility, electrolyte and deposition capacity.^{48,50–52} Another critical influence on the Na dendrite formation is the solid electrolyte interphase (SEI). Generally, the SEI layer is formed at the interface between liquid electrolyte (LE) and Na metal anode due to the decomposition of organic electrolyte components on the surface of reactive Na metal.⁵³ A good SEI layer is considered to be electronically insulating but ionically conductive,

which will block further side reactions between LE and Na metal while transporting Na⁺ during electrochemical cycling. However, an unstable SEI layer will lead to non-uniform Na⁺ flux, resulting in Na dendrite growth. The accumulation of sharp Na dendrites may penetrate through the separator, causing safety concerns over internal short circuits. (2) Low Coulombic efficiency (CE) and poor cycling performance. An unstable SEI layer will not only cause Na dendrite growth, but also lead to the depletion of electrolyte and electroactive Na during the repeated breakage and repair of the SEI layers during cycling. The consumption of the electrolyte and Na metal will lower the CE and also shorten the life time. Meanwhile, the accumulation of “dead Na” will give rise to large voltage polarizations and increase the resistance of the batteries. (3) Infinite volume changes. The host-less nature of the Na metal anode results in infinite volume changes during repetitive Na plating/stripping processes.

The challenging issues associated with metallic Na anode have also been noticed in practical NMBs. The undesired Na dendrite growth had been observed by Hartmann *et al.* in the Na–O₂ battery system.⁵⁴ The porous structure of Na dendrites composed of sodium and oxygen can also be found in the holes of the separator. Another group also reported similar Na dendrite growth in Na–O₂ batteries with different discharge capacities.⁵⁵ It has now come to attention that the performance of Na–O₂ batteries is not only dependent on the cathode, but also the Na metal anode, which is also a key component that can affect the life time and stability of Na–O₂ cells.

In the initial studies on NMBs, researchers put more emphasis on the development of other cell components, such as cathode materials and electrolyte. The important role of the Na metal anode had been significantly neglected. However, the importance of Na metal anode has been highlighted in recent years and many creative studies have provided possible solutions to address the issues of Na metal. With this in mind, a comprehensive summary is required for a deep understanding on the recent progresses of Na metal anodes, particularly for NMBs. Although this topic has been partially mentioned in an excellent review paper focusing on Li metal anodes, the progress and challenges associated with Na metal anodes has yet to be summarized in detail.⁵⁶ Thus, on the basis of this motivation, this review article focuses on the recent developments of metallic Na anodes, including the fundamental understanding, novel characterization methods, and strategies for protection and future perspectives. Our review will accelerate further improvement and application of Na metal anodes from fundamental studies to practical application in NMBs.

2. The fundamentals of Na dendrite formation

2.1 Properties of Na dendrites

Over the past decades, there have been numerous studies on the formation of Li dendrites, their growth process, surface, and interface chemistry. However, unlike the systematic investigations of the Li anode and Li dendrites,^{51,57–60} very little

research has focused on the properties and process of Na dendrite growth. Belonging to the same group of alkali metals as Li, metallic Na is expected to follow similar principles and mechanisms during electrochemical processes. However, the properties of Na metal are still slightly different from Li metal, which will affect the Na dendrite growth. Fig. 1(a) shows the various properties of metallic Na and Li in terms of atomic, physical and mechanical properties. It can be seen that these two alkali metals present different electronic structures and atomic properties. Furthermore, the Na metal intrinsically displays higher chemical activity and lower mechanical properties.

To gain a better understanding on the difference between Na and Li dendrites, Hong *et al.* carried out an *in operando* experiment to study the chemical, mechanical and electrochemical stability of Li and Na dendrites under quasi-zero electrochemical field (QZEF).⁶¹ Generally, QZEF refers to electrochemical systems where the external electrochemical process is halted, such as the completion of charge/discharge, interruption of battery operation and massive battery decay under abuse. In their work, similar electrolytes of 1 M LiPF₆ in dimethyl carbonate (DMC)/ethylene carbonate (EC) and 1 M NaPF₆ in DMC/EC were used for Li and Na, respectively. Firstly, both Li and Na dendrites were deposited on the Li and Na electrode under the same condition. To investigate the effects of electrolytes on the dendrites, both electrodes were allowed to settle under QZEF. Interestingly, the Li dendrites showed almost no change under QZEF, but the Na dendrites were gradually dissolved and diminished when settling in electrolyte. Furthermore, a large portion of the Na dendrites had disappeared after 6 h. Secondly, two pieces of fresh Li and Na foils were soaked in the electrolyte to study the chemical stability. The results indicated that the surface of the soaked Na foil possessed rough pits and heaves due to the high activity of Na metal. Thirdly, the mechanical stability of the Li and Na dendrites and their SEI layers were investigated *via*

applying mechanical forces, as shown in Fig. 1(b). It can be observed that the Li dendrites and their SEI layers are more mechanically stable than Na dendrites due to the robust chemical bonding and lower chemical activity. The weakened mechanical properties of Na dendrites are a critical problem because it can lead to the ceaseless dissolution and damaging of Na dendrites and the development of new SEI, which causes NMBs to have irreversible capacity loss and shortened life times. Lastly, the electrochemical performances had also been investigated using Li–Li and Na–Na symmetric cells. Generally, the Na–Na cells possessed more pronounced voltage hysteresis fluctuations during repeated plating/stripping compared to Li–Li cells, which was attributed to the unstable SEI layer in the similar electrolyte systems.

In comparison to Li metal, Na dendrites and their related SEI layers are more sensitive to the electrolyte and external environments. In this case, achieving a stable SEI layer and reducing Na dendrite growth will be more challenging compared to the problems associated with Li metal anodes.

2.2 Advanced techniques for the study of Na dendrites

Similar to the studies on Li dendrites, advanced techniques for the characterizations of Na dendrite growth and SEI layers are necessary to gain a deep understanding on their fundamental mechanisms and properties.⁶² In general, regular techniques have been used to study the Na dendrite and SEI formation, including scanning electron microscopy (SEM), optical microscopy, X-ray photoelectron spectroscopy (XPS), Time-of-flight secondary ion mass spectrometry (TOF-SIMS) and several other methods. It is worth mentioning that our group firstly demonstrate the Rutherford Backscattering Spectrometry (RBS) technique to study the SEI formation on Na metal anodes, which is a very powerful tool to exhibit the compositions and thickness of the SEI layers formed during electrochemical cycling.

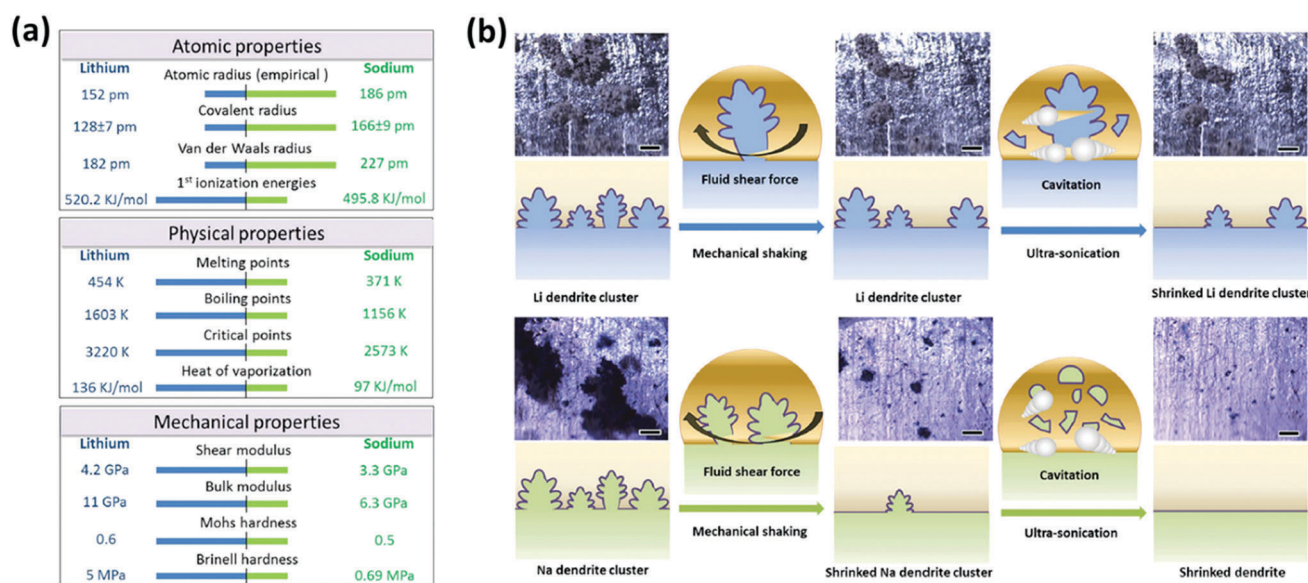


Fig. 1 (a) Various properties of Li and Na; (b) mechanically stability under quasi-zero electrochemical field for Li and Na dendrites.⁶¹ Reproduced with permission from Elsevier.

Apart from the *ex situ* techniques, advanced *in situ* techniques are considered to be more promising for observing the plating/stripping behaviors and dendrite growth process of Na metal. Rodriguez *et al.* demonstrated the *in situ* optical imaging of the Na deposition process, as shown in Fig. 2(a).⁶³ Three types of electrolytes (1 M NaPF₆ in (i) EC/diethyl carbonate (DEC); (ii) propylene carbonate (PC)/fluoroethylene carbonate (FEC); (iii) FEC/DEC) are used for their home-made hermetically sealed optical cell. From observation of the *in situ* optical images, highly porous Na with mossy and dendritic structures were deposited for all the electrolytes. Meanwhile, the Na dendrites formed in both EC/DEC and PC/FEC were easily expelled into the electrolyte along with gas generations. However, it has also been demonstrated that the issues of porous depositions, gas evolutions and Na loss were reduced when using FEC as the co-solvent.

In situ atomic force microscopy (AFM) is another useful analytical technique that can provide visualized evidence of electrochemical reactions in batteries system, particularly for changes in surface morphology of the electrode. Recently, Chen's group reported an *in situ* AFM study of Na deposition on a homemade planar electrode in a carbonate-based electrolyte. The schematic of the *in situ* AFM setup is shown in Fig. 2(b).⁶⁴ In their design, the *in situ* AFM included a gold coated homemade planar electrode, a sodium electrode, an O-ring for sealing of the liquid, an AFM probe and an optical camera. They firstly studied the Na deposition behavior by *in situ* AFM using an electrolyte consisting of 1 M NaClO₄ in EC/PC (1:1 v). Three stages were visualized in the deposition processes by *in situ* AFM combined with optical images. The first stage was the nucleation step appearing in the beginning of Na deposition (100 s). After 300 s deposition, the growth of Na was clearly observed. Subsequently, the Na continues to spread and finally formed a

rough layer after 1000 s, followed by the formation of Na dendrites and dead Na layers. FEC was further used in their study as an additive in the electrolyte, which can stabilize the Na deposition and suppress the Na dendrite formations. From the *in situ* AFM, the FEC-containing electrolyte demonstrated a more homogeneous morphology and higher modulus than those in the pristine electrolytes. Their work provides a good example of the development of *in situ* strategies to study the Na metal anode.

In situ nuclear magnetic resonance (NMR) spectroscopy is used as a unique and indispensable tool for the nondestructive analysis of battery systems. In previous studies, *in situ* NMR has given valuable and quantitative insight with adequate temporal resolution to analyze the Li microstructure (dendritic and mossy Li). Grey and colleagues firstly demonstrated *in situ* ²³Na NMR on a Na metal electrode during electro-deposition of Na (Shown in Fig. 2(c)).⁶⁵ Consistent with the phenomenon observed from other techniques, a high surface area morphology was produced in the continuous galvanostatic plating of Na. Through the use of *in situ* ²³Na NMR, it could be observed that the two cells cycled with higher current densities (1 and 2 mA cm⁻²) exhibited similar behavior in terms of their efficiency in removal of the high surface area microstructures. In contrast, a different behavior was seen for the lowest current density studied (0.5 mA cm⁻²), where the efficiency of removal is dramatically increased. Their study suggested that these two regimes are distinguished by both the efficiency in which high surface area deposits can be removed and the time dependence of the nucleation process, both of which are greater at lower current.⁶⁵

The techniques discussed above are suitable to study Na dendrite growth under relatively large scales (micro size), however, the nucleation process of Na deposition is still difficult to be determined. Li *et al.* presented the first nanoscale-resolution observation of electrochemical Na plating/stripping dynamics

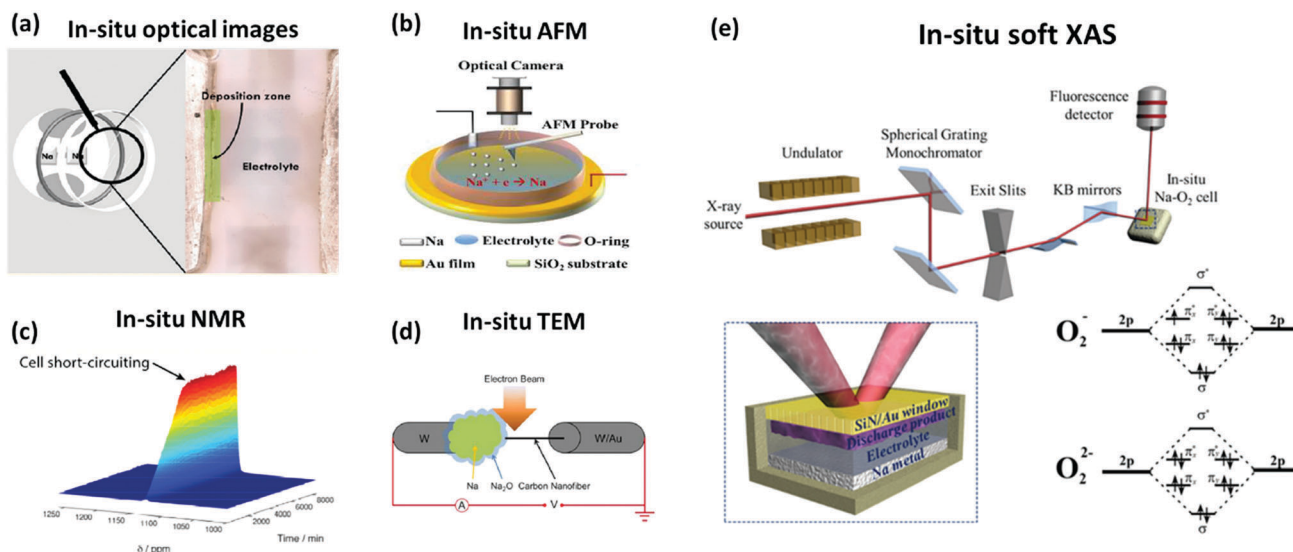


Fig. 2 Different analytical techniques for Na deposition (plating) studies: (a) *in situ* optical images.⁶³ Reproduced with permission from American Chemical Society. (b) *In situ* AFM.⁶⁴ Reproduced with permission from The Royal Society of Chemistry. (c) *In situ* NMR.⁶⁵ Reproduced with permission from American Chemical Society. (d) *In situ* TEM.⁶⁶ Reproduced with permission from Elsevier. (e) *In situ* soft XAS.¹³⁶ Reproduced with permission from The Royal Society of Chemistry.

via in situ electron microscopies using amorphous carbon nanofibers (CNF) as a current collector.⁶⁶ Fig. 2(d) shows their set up for the *in situ* transmission electron microscope (TEM) and SEM. From the *in situ* SEM and TEM, it was found that the Na metal is grown and dissolved reversibly as nano/microparticles at all possible locations around individual CNFs and even throughout their network. Interestingly, Na ions were also transported in the fibers, enabling a more homogeneous Na deposition deep into the interior network. Their works provide some new insights and technical paths in the design of dendrite free Na metal anodes.

Synchrotron-based Soft X-ray absorption spectroscopy (XAS) can reveal the surface and interface information about the local electronic and chemical structure of products by probing states near the Fermi level using X-rays. More recently, our group develop, for the first time, an *in situ* system for soft XAS study of non-aqueous Na–O₂ cells to examine the degradation mechanism of discharge products (see Fig. 2(e)).¹³⁶ It was discovered that a non-uniform layer of side-products formed on the surface of NaO₂ due to the decomposition reaction between the discharge product and electrolyte. Furthermore, we have exemplified the capability of the *in situ* soft XAS technique in illuminating the underlying mechanisms of electrochemical processes benefiting from the elemental selectivity and chemical sensitivity. We also believe that *in situ* soft XAS is a promising tool to study the electrochemical plating/stripping and SEI formation of the Na metal anode, which will be demonstrated in the future works.

As an alternative method of analyzing the Na deposition process, Kondou *et al.* studied the Na plating procedure in another view by investigating the thermal reactivity of Na metal.⁶⁷ From their results, the heat flow profile of sodium plating exhibited lower peak intensities and larger widths without FEC additive. On the other hand, with FEC, the heat flow profile dramatically changed, exhibiting a three-fold increase in peak intensity compared to the FEC-free electrolyte.⁶⁷

As seen above, many advanced characterization techniques, especially the *in situ* techniques, have been proposed to understand the growth of Na dendrites and SEI layer formation. Unlike the detailed studies for Li anodes, many fundamental questions have yet to be answered for the Na metal anode and its dendrite growth, which will be discussed in the perspective sections. Meanwhile, any one of these techniques alone is not enough to gain a deep and comprehensive understanding on the surface and interface chemistry of the Na metal anode and its SEI layers, which will require the combination of different analytical techniques in future research. New approaches, such as synchrotron radiation-based techniques, are expected to provide new insight and guidance on the surface chemistry of Na metal anodes.

3. Stabilization of the SEI layer on Na metal anodes

3.1 Electrolyte modification for stable SEI

As discussed above, the SEI layer is one of the most important components of the Na metal anode. An ideal SEI should possess

high ionic conductivity, sufficient density, small thickness and high flexibility to mechanically suppress the Na dendrite growth.^{60,62,68} During electrochemical cycling, the major components of the SEI layer are generated from the reduction of solvents and salts in the organic electrolytes. Thus, the properties of SEI layer are always determined by the organic solvent, Na salt and additives in the electrolytes.⁶⁹

FEC has already been proven as an effective additive to stabilize the SEI on Li metal surfaces, and has also been proposed for Na anodes.⁷⁰ In the last section, Rodriguez *et al.* and Chen's group used FEC as an additive to demonstrate their different *in situ* techniques for Na deposition. Tarascon's group also demonstrated that the use of FEC as an additive minimizes the irreversible capacity of Na-half cells using Na metal as the anode.⁷¹ From their study, FEC can limit the Na reactivity toward the electrolyte *via* the growth of a protective layer with an impedance that increases with time. This protective layer mainly consisted of a harder and more homogeneous NaF interface.⁶⁴ The NaF coating can provide a homogeneous Na⁺ flux to the surface of the electrode, resulting in reduced Na dendrite growth and longer life times. More recently, Wang *et al.* reported a bi-functional electrolyte additive of potassium bis(trifluoromethylsulfonyl)imide (KTFSI) to stabilize Na metal electrodes.⁷² In their design, the K⁺ cations are preferentially adsorbed on the deposited Na and provide electrostatic shielding to suppress dendritic deposition. With the assistance of the bi-functional electrolyte additive, the Na metal anode could realize a long cycle life over hundreds of hours at a high capacity of 10 mA h cm⁻².

The concentration of the salt in electrolyte will also affect the cycling efficiency of Na metal anodes.^{73,74} Lee *et al.* presented an ultra-concentrated electrolyte composed of sodium bis(fluoro-sulfonyl)imide (NaFSI) in 1,2-dimethoxyethane (DME) for Na metal anodes coupled with high-voltage cathodes.⁷⁵ Fig. 3(a) compares the CE for Na plating/stripping on stainless steel (SS) with different concentrations of salt in the electrolyte. Higher concentration NaFSI-DME electrolytes led to substantially improved initial CE for Na plating/stripping. Moreover, with the 5 M NaFSI-DME electrolyte, a high CE of 99.3% was obtained for 120 cycles at a rate of C/10. Meanwhile, the rate performances (Fig. 3(a)) had also been drastically enhanced with a CE of 93.8% at a high rate of 2C using 5 M NaFSI-DME electrolyte compared to the conventional dilute 1 M NaPF₆-EC/PC electrolyte. However, the highly concentrated electrolyte still possesses shortfalls, such as high viscosity, poor wettability, and high salt cost. In this case, Zheng *et al.* demonstrated the use of a hydrofluoroether as an "inert" diluent can significantly reduce the salt concentration as well as maintain the high CE.⁷⁶ With their design, a relatively low salt concentration (2.1 M NaFSI/DME-bis(2,2,2-trifluoroethyl)ether (1 : 2)) enabled the dendrite-free Na deposition with a high CE of >99% and greatly enhanced the fast charging (20C) and stable cycling (90.8% after 40 000 cycles) of Na||Na₃V₂(PO₄)₃ batteries. The bis(2,2,2-trifluoroethyl)ether diluent will not break the localized Na⁺-FSI⁻-DME solvation structures but improve the interfacial reaction kinetics and interfacial stability of the Na metal anode. Their work has

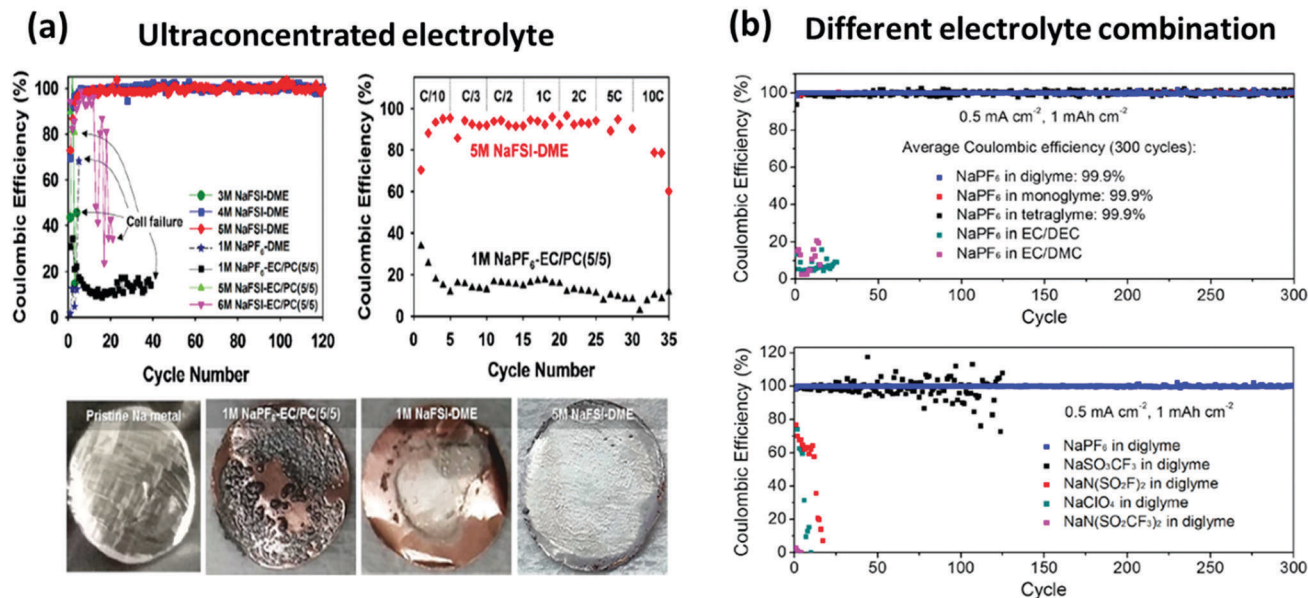


Fig. 3 (a) Coulombic efficiency of Na plating/stripping in Na/SS cells and photographs of a pristine Na metal electrode and Cu substrates after the initial Na plating with different concentration of electrolytes.⁷⁵ Reproduced with permission from American Chemical Society. (b) Plating–stripping Coulombic efficiencies of Na metal anodes cycled using (a) 1 M NaPF₆ in various electrolyte solvents and (b) 1 M of various electrolyte salts in diglyme.⁷⁷ Reproduced with permission from American Chemical Society.

opened a new avenue to tailoring of the electrolyte chemistry with low salt concentrations for developing high-performance NMBs.

It is known that the combination of different electrolyte components, such as the solvent and salt, will further affect the Na deposition behaviour. In 2015, Cui's group gave a comprehensive study on the electrolyte combinations using different electrolyte salt of NaPF₆, NaN(SO₂CF₃)₂ (NaTFSI), NaFSI, NaSO₃CF₃ (NaOTf) and NaClO₄ with solvents such as monoglyme, tetraglyme, EC/DEC and EC/DMC.⁷⁷ Fig. 3(b) presented the plating–stripping CE of Na metal anodes cycled using 1 M NaPF₆ in various electrolyte solvents and 1 M of various electrolyte salts in diglyme, respectively. Generally, the electrolytes of 1 M NaPF₆ in glymes (mono-, di- and tetraglyme), can enable the highest reversibility and no dendrite structures at room temperature. The SEI formations were also studied using depth profile XPS, in which the uniform inorganic SEI layer made of Na₂O and NaF are highly impermeable to electrolyte solvent and conducive to dendrite inhibition.

Other than the conventional electrolytes, significant efforts have been made to develop novel electrolyte systems to achieve high CE and dendrite-free Na depositions. Song *et al.* reported a dendrite-free Na-metal electrode employing a non-flammable and highly Na⁺-conductive NaAlCl₄·2SO₂ inorganic electrolyte with enhanced electrochemical performances compared to the conventional organic electrolytes. These remarkable performances can be attributed to the unique nature of the highly concentrated SO₂-based inorganic electrolyte and its intrinsically high Na⁺ conductivity.⁷⁸ Subsequently, another novel highly concentrated sodium electrolyte based on liquid ammonia has been reported, which can be described as NaY·xNH₃ (Y: I⁻, BF₄⁻, BH₄⁻).⁷⁹ These electrolytes showed excellent properties such as low flammability and high specific ionic conductivity

with dendrite-free and highly reversible Na plating/stripping behaviours as well as high CE when performed on a Cu substrate.

In this section, we summarized the recent research progress focusing on the modification of electrolyte components to obtain stable SEI layers for Na metal anodes (Table 1). The promising approaches can be classified as: (1) the rational combination between salt and solvent in the electrolytes, which plays an important role in the electrochemical performances. It is considered that the use of NaPF₆ as salt and glymes as solvent will create a uniform inorganic SEI layer consisting of Na₂O and NaF, leading to both dendrite-free deposition and long cycling life. (2) The ultra-high salt concentration in the electrolyte can provide remarkable effects to suppress the Na dendrite growth and achieve stable SEI formation. The “inert” diluents in the electrolyte can not only decrease the salt concentrations, but also maintain the excellent plating/stripping behaviours. (3) FEC is widely accepted as the most effective electrolyte additive to produce a stable NaF SEI layer and improve the CE. (4) Beyond the existing electrolytes, novel electrolyte systems with the advantages of low cost, improved safety as well as dendrite-free Na depositions are expected to address the current issues in NMBs.

3.2 Artificial SEI layers by surface modification

In addition to the *in situ* formed SEI layer from the reaction between metallic Na and electrolyte, surface modification with artificial SEI layers is considered as another effective strategy to protect Na metal anodes. The artificial SEI is fabricated prior to cell assembly and can block the direct contact between Na metal and LE, thus preventing the consumption of the electrolytes and electrode materials, heterogeneous deposition, and dendrite formation.⁴⁸ Compared to the *in situ* formed SEI from

Table 1 Summary of the reported literature on electrolyte modification for stable Na metal SEI formation

Na cells	Electrolyte salt	Electrolyte solvent	Additives	Current density (mA cm ⁻²)	Capacity (mA h cm ⁻²)	CE/life time	Ref.
Na–Cu	1 M NaPF ₆	Diglyme	—	0.5	1	99.9% (300 cycles)	77
	1 M NaPF ₆	Monoglyme	—	0.5	1	99.9% (300 cycles)	
	1 M NaPF ₆	Tetraglyme	—	0.5	1	99.9% (300 cycles)	
	1 M NaPF ₆	EC/DEC	—	0.5	1	<20% (<25 cycles)	
	1 M NaPF ₆	EC/DMC	—	0.5	1	<20% (<25 cycles)	
	1 M NaN(SO ₂ CF ₃) ₂	Diglyme	—	0.5	1	<10% (<25 cycles)	
	1 M NaFSI	Diglyme	—	0.5	1	<10% (<25 cycles)	
	1 M NaSO ₃ CF ₃	Diglyme	—	0.5	1	<80% (<125 cycles)	
	1 M NaClO ₄	Diglyme	—	0.5	1	<10% (<25 cycles)	
	Na–Na	NaAlCl ₄ ·2SO ₂	—	—	0.75	1.5	
Na–Cu	4 M NaFSI	DME	—	0.2	0.2	99% (300 cycles)	73
	4 M NaFSI	DME	—	0.5	0.5	99% (300 cycles)	
	4 M NaFSI	DME	—	1	1	99% (300 cycles)	
Na–Al	4 M NaFSI	DME	—	0.5	0.5	99% (300 cycles)	
Na–Na	1 M NaPF ₆	EC _{0.5} DMC _{0.5}	3% FEC	0.05	—	600 h	71
Na–SS	5 M NaFSI	DME	—	C/10	—	99.3% (120 cycles)	75
Na–Na	5 M NaFSI	DME	—	0.0028	0.0014	600 h	
Na–Cu	NaI·3.3NH ₃	—	—	10	—	580 h	79
Na–Cu	1.7 M NaFSI	DME	—	0.2	1	<50% (<50 cycles)	76
	1 M NaPF ₆	EC-DEC	—	0.2	1	<25% (<50 cycles)	
	5.2 M NaFSI	DME	BTFE	0.2	1	>99% (400 cycles)	
	1.5 M NaFSI	DME	BTFE	0.2	1	>99% (400 cycles)	
	2.1 M NaFSI	DME	BTFE	0.2	1	>99% (400 cycles)	
	3.1 M NaFSI	DME	BTFE	0.2	1	>99% (400 cycles)	
	2.1 M NaFSI	DME	BTFE	1	1	>950 h	
Na–Na	2.1 M NaFSI	DME	BTFE	2	1	>950 h	
Na–Cu	1 M NaPF ₆	EC/PC	FEC	1	1	100 h	64

the electrolyte components, the artificial SEI possesses more advantages: (1) as discussed in 2.1, the highly chemically active Na metal can react with electrolyte components spontaneously. With the protection of artificial SEI, these side reactions can be effectively blocked. (2) The properties of the artificial SEI can be easily regulated and tailored without any effect from the electrochemical process. Thus, the development of artificial SEI layers has grown very fast in the past year and will be discussed in this section.

To provide guidance for the development of suitable protective films on Na metal anodes, Tian *et al.* carried out a comprehensive theoretical study on both diffusion and mechanical performance of layered materials to reveal their possibilities as artificial SEI layers for Na metal anodes.⁸⁰ From the simulation results, the introduction of defects, the increase of bond length, and proximity effect can improve the conductivity of Na⁺ ions and enable lower diffusion barriers with higher diffusion rates.⁸⁰ Generally, the materials with puckering structure, such as phosphorene, SnS, and SnSe, are not good for Na⁺ ion diffusion, and even worse for the strain properties, making them not suitable as artificial protection coatings. Meanwhile, defective h-BN or graphene are also not suitable for Na metal anodes due to the larger radius of Na⁺ resulting in difficult diffusion of Na within the structures. Nevertheless, the simulation results show that both silicene or Si materials are potentially promising artificial SEI coatings for Na metal with relatively high Na diffusion rate and stiffness stronger than common SEI films.⁸⁰ Furthermore, another group screened the Open Quantum Materials Database to identify various coatings exhibiting chemical equilibrium with the Na metal anode.⁸¹ They identify 118 promising coatings for Na metal anode

including binary, ternary, and quaternary compounds, which are listed in their paper.

In the latest studies, different approaches have been proposed to fabricate artificial SEI or protective layers for Na metal anodes. Among them, gas phase deposition methods, especially atomic layer deposition (ALD), has attracted increasing attention. ALD is a thin film deposition technique which is based on the sequential use of self-limiting gas–solid reactions.^{82,83} It has the exclusive advantages of extremely uniform and controllable deposition at low deposition temperatures.^{84,85} It has been widely studied as a novel surface coating and modification approach for alleviating side reactions and improving electrochemical performances, even enhancing the thermal stability of both anode and cathode materials.^{86–88} Meanwhile, ALD Al₂O₃ coatings have been verified as effective artificial SEI coatings for Li metal anode by different groups.^{89,90} Recently, our group and Hu's group reported the applications of ALD and plasma enhanced ALD Al₂O₃ coatings as protective layers for Na metal anodes, respectively.^{91,92} The ALD Al₂O₃-coated Na anode presented a large improvement in the electrochemical plating/stripping performances and the suppression of Na dendrite growth in both carbonate-based and ether-based electrolytes. Fig. 4(a) presents the comparison of the cycling stability of the Na@25Al₂O₃ and the bare Na foil at a current density of 3 mA cm⁻² and 5 mA cm⁻² with the capacity of 1 mA h cm⁻² from our work. The results showed that the Na metal with ALD Al₂O₃ coating displayed much more stable performances with almost no change in polarization at different current densities. As mentioned above, we firstly demonstrated the advanced RBS measurement in this paper to study the SEI formation with ALD Al₂O₃ coating. Fig. 4(b) exhibits the RBS spectra and calculated

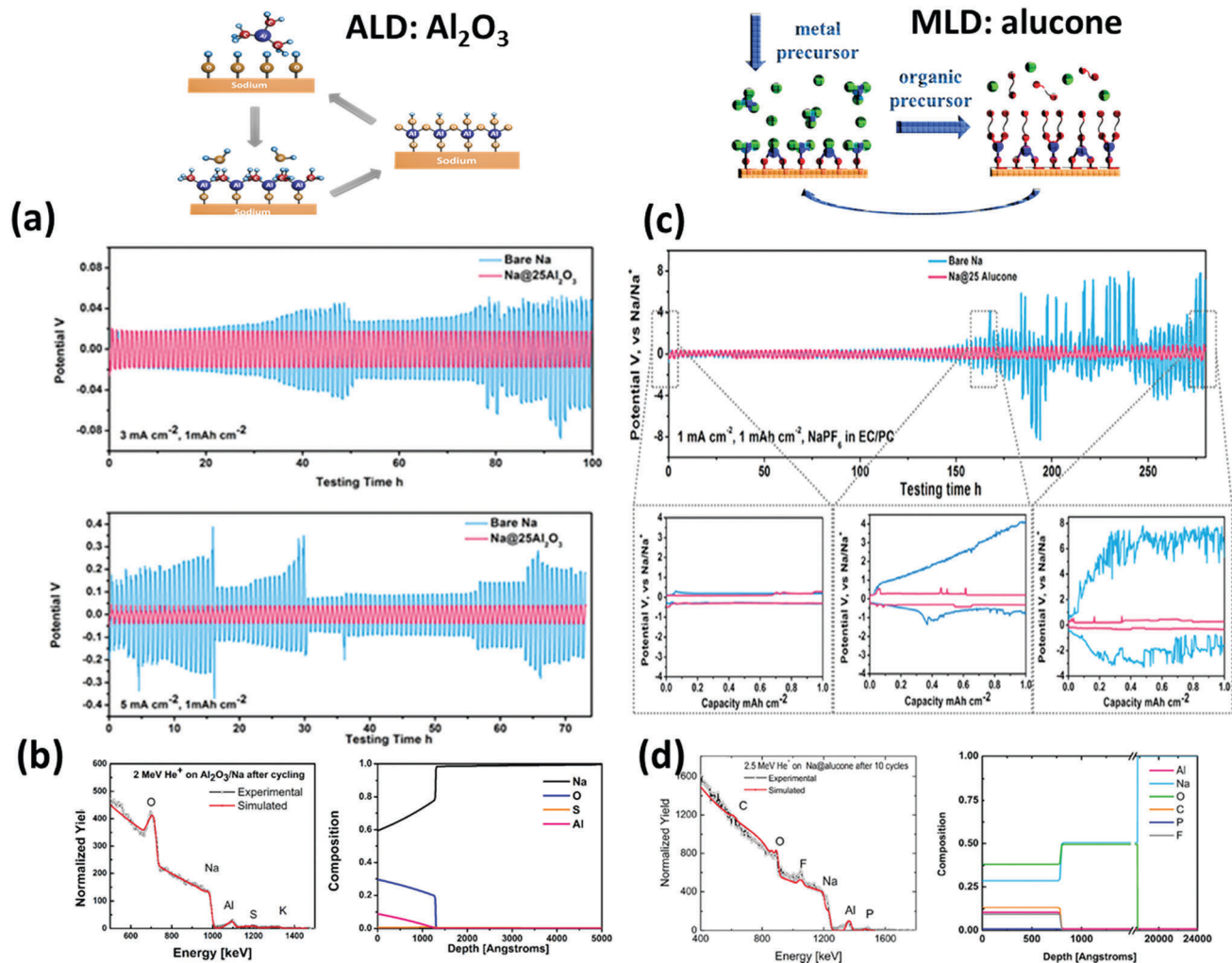


Fig. 4 ALD Al₂O₃ coating as protective layer for Na metal anode: (a) electrochemical cycling and (b) RBS spectra and calculated depth profiles of Na@25Al₂O₃ after cycling; MLD alucone coating as a protective layer for Na metal anode;⁹² reproduced with permission from John Wiley and Sons. (c) Electrochemical cycling and (d) RBS spectra and calculated depth profiles of Na@25 alucone after cycling.^{93,98} Reproduced with permission from American Chemical Society.

depth profiles of Na@25Al₂O₃ after cycling. From the RBS analysis, $\sim 85 \pm 5\%$ of the as-deposited Al remained on the surface of Na metal, indicating the electrochemical stability of ALD Al₂O₃ in ether-based electrolyte. Meanwhile, the sulfur areal density was larger by a factor of two for the bare Na sample compared to Al₂O₃-coated Na, demonstrating the effective prevention of side reactions between Na metal and electrolyte.⁹²

As an extension of ALD, molecular layer deposition (MLD) has been further developed by replacing the oxidizing precursor with organic linkers or the addition of molecular fragments into the film to form the polymer and organic-inorganic hybrid films.⁹³ The MLD films provide increased toughness and flexibility as a result of C-C and C-O bonds from the organic linkers, which is reported to enhance the electrochemical performances of Si anodes, Li metal anodes and S cathodes.⁹⁴⁻⁹⁷ Our group firstly demonstrated the application of MLD alucone (Al-ethylene glycol (EG)) as a protecting layer for Na metal anode cycled in carbonate-based electrolyte (NaPF₆ in EC/PC).⁹⁸

Fig. 4(c) shows the comparison of the cycling stability of the Na@25 alucone and the bare Na foil at a current density of 1 mA cm⁻² with the capacity of 1 mA h cm⁻². From the results, the Na@25 alucone presented improved plating/stripping performances with reduced dendrite growth and double the life time. Meanwhile, the RBS technique was also carried out to study the surface changes during cycling, as shown in Fig. 4(d). From the RBS results, the Al peaks and associated depth profiles do not change dramatically after cycling, indicating the chemical and electrochemical stability of MLD alucone in the NaPF₆ contained electrolyte. In comparison, the Na@Al₂O₃ had also been investigated in this electrolyte (NaPF₆ in EC/PC), which showed improved performances compared with bare Na. However, it was still not comparable to the MLD alucone-coated Na metal anode. From our works, we have demonstrated that both ALD and MLD are effective tools to deposit artificial SEI layers with controllable thicknesses under relatively low temperatures. The as-deposited ALD/MLD films exhibit excellent electrochemical

stability and are effective in suppressing Na dendrite formation through forming robust artificial SEI layers.

Additionally, chemical reactions with Na metal is another approach to fabricate an artificial SEI on the surface. In other words, Na metal is used as a reactant to form the artificial SEI. Archer's group firstly demonstrated the reaction of metallic Na with bromopropane to undergo the Wurtz reaction as illustrated in the Fig. 5(a).⁹⁹ In doing so, NaBr is formed on the surface of Na foil with thicknesses ranging from 2–12 μm . Fig. 5(a) shows the galvanostatic cycling performance of Na/NaBr and control samples at the current density of 0.5 mA cm^{-2} with the capacity of 0.5 mA h cm^{-2} . From the results, the cell comprising NaBr-coated Na was stable for at least 250 h with minimal rise in cell polarization, producing nearly a 10-fold improvement in the cell lifetime. Furthermore, the *in situ* visualization was performed to contrast the electrodeposition stability with and without NaBr layers on the sodium anode. The results showed that the NaBr coating not only restricts dendritic formation, but also prevents unwanted side reactions between the electrode and electrolyte.⁹⁹ Afterwards, their group reported ionic membranes synthesized on a metallic Na anode by an *in situ* electro-initiated polymerization method of imidazolium-type ionic liquids containing unsaturated functional groups,

as shown in Fig. 5(b).¹⁰⁰ The study showed that the ionic membranes can protect the Na metal against parasitic reactions with liquid electrolyte without compromising ion transport in the SEI. The ionic membrane-protected Na anodes exhibited high CE and stable long-term cycling even at relatively high current densities. Meanwhile, the ionic membranes can reduce the electric field on the surface of Na, resulting in the uniform deposition of Na metal. From their works, the reaction-based method using Na metal as reactant has been proven as a promising alternative strategy to synthesizing artificial SEI layers on the Na metal surface. However, it is still believed that the thickness control is the main challenge for this method in term of unpredictable chemical reactions on the Na surface.

Other approaches have also been reported to modify the surface of Na or create artificial SEI layers for Na metal anodes. Kim *et al.* demonstrated a multistep approach to fabricate a free-standing composite protective layer that could enable enhanced reversibility of Na metal anode by mechanically suppressing Na dendrite growth and mitigating the electrolyte decomposition.¹⁰¹ In this work, the as prepared free-standing composite protective layer was laminated on the Na metal electrode by roll-pressing. One of the key factor in their protective layer was the high mechanical strength and high ionic conductivities.

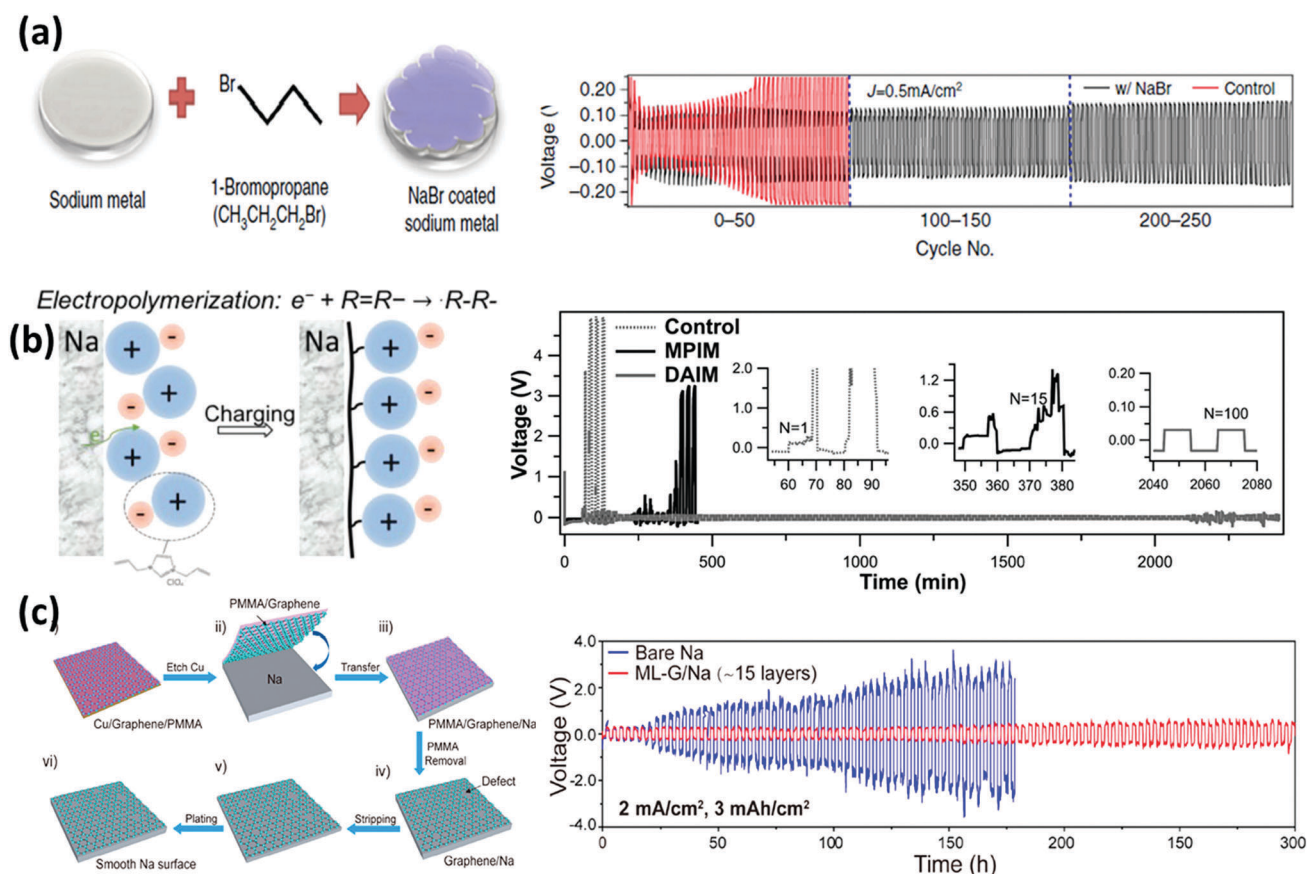


Fig. 5 (a) Schematic showing the procedure used to coat Na with NaBr and its electrochemical performances.⁹⁹ Reproduced with permission from Springer Nature. (b) A schematic drawing of the polymeric ionic liquid film formation on Na and its electrochemical performances.¹⁰⁰ Reproduced with permission from John Wiley and Sons. (c) Schematic diagram showing the fabrication process of graphene-coated Na and its electrochemical performances.¹⁰¹ Reproduced with permission from American Chemical Society.

Similar ideas have been proposed using ultrathin graphene films as the free standing protective layer on Na metal anode, as shown in Fig. 5(c).¹⁰² Interestingly, the Na anode stability at different current densities and capacities was dependent on the thickness of the graphene film. To achieve an optimal performance, the thickness of the graphene film was meticulously selected based on the applied current density. It was found that 15 layers of graphene (~ 5 nm) can significantly enhance the Na cycling behavior at a high current density of 2 mA cm^{-2} and a capacity of 3 mA h cm^{-2} over 100 cycles. The stable Na metal anode with a high cycling capacity of 3 mA h cm^{-2} is more promising in terms of the practical application of NMBs. Another interesting work has been reported by Li and colleagues.¹⁰³ In their study, they used a commercial carbon paper (CP) as the protection layer for Na metal anode, in which the CP directly covered the surface of Na foil. The Na anode with CP exhibited significantly improved over-potentials and cycling stability (up to ~ 1200 cycles). This positive effect was attributed to the large surface area of carbon paper that is capable of dissipating current density and its less reactive surface favoring the formation of a stable SEI layer.¹⁰³

In this part, we have given an overview of the recent developments of the various surface modifications strategies for the protection of Na metal anodes, as summarized in Table 2. Based on the fabrication process, the methods can be categorized into the following: (1) the chemical/physical deposition method (like ALD and MLD). These deposition methods exhibit the advantages of uniform coverage and precise control over film thickness. In the future, novel coating materials with high Na^+ conductivity are expected to be developed for Na metal anode by these methods. (2) Reaction method using Na as a reactant. From this process, Na-containing materials or ionically conductive layers can be obtained. However, control over the desired thickness and a deep understanding on the surface/interfacial change are still lacking. (3) The mechanical transfer method. Based on this method, a larger variety of materials can be explored

with a facile fabrication process. However, the Na metal anode and these protective layers are usually connected by physical contact, which is not as strong as the chemical bonding used by the other two methods.

4. Nanostructured Na metal anodes

4.1 Nanostructured current collectors

Because the spatial inhomogeneity of the Na^+ distribution on an electrode surface contributes directly to the Na dendrite formation, it is urgent to develop strategies to produce a uniform Na^+ flux.^{50,104} One of the most popular approaches is to increase the surface area of the electrode to dissipate the local current density, which can be realized by manipulating the nanostructure of the current collectors. Al foil, the typical current collector for cathode materials in LIBs, can also serve as a current collector for the anodes in NIBs and NMBs because it will not alloy with Na. However, Na dendrites will be formed on the Al foil due to the inhomogeneous distribution of local current. To achieve dendrite-free Na deposition, a nucleation layer was produced on the Al foil to assist the sodium seeding process with a lower nucleation energy barrier and improved structure for stable sodium plating.¹⁰⁵ The results showed that over 1000 plating–stripping cycles with an average CE of 99.8% was maintained with a low average hysteresis of 14 mV and smooth Na film deposited on the Al current collector. Furthermore, this Na metal-free anode coupled with a pre-sodiated pyrite cathode could provide an energy density of $\sim 400 \text{ W h kg}^{-1}$, which is very promising for future applications. Beyond planar Al foil, Luo's group reported porous Al foil as the Na plating substrate to suppress the Na dendrite growth.¹⁰⁶ Fig. 6(a) illustrates the schematic of Na deposition on planar and porous Al foils and the SEM images of porous Al foils before and after cycling. From the SEM images, it can be observed that the Na plated on porous Al was homogeneously distributed on the

Table 2 Summary of the reported literature on surface modification techniques for stable Na metal anodes

Na cells	Coating materials	Electrolyte	Current density (mA cm^{-2})	Capacity (mA h cm^{-2})	CE/life time	Ref.
Na–Na	NaBr	1 M NaPF ₆ in EC/PC	0.25	0.25	250 cycles	99
		1 M NaPF ₆ in EC/PC	0.5	0.5	250 cycles	
		1 M NaPF ₆ in EC/PC	1	1	250 cycles	
Na–Na	Inorganic–organic composite protective layer	1 M NaClO ₄ in EC–PC	0.5	1	> 550 h	101
Na–Na	ALD Al ₂ O ₃	1 M NaClO ₄ in EC–DEC	0.25	1	400 h	91
		1 M NaClO ₄ in EC–DEC	0.5	1	120 h	
Na–Na	ALD Al ₂ O ₃	1 M NaCF ₃ SO ₃ in DEGDME	3	1	500 h	92
Na–Na	MLD alucone	1 M NaPF ₆ in EC/PC	1	1	270 h	98
		1 M NaPF ₆ in EC/PC	3	1	120 h	
Na–Na	Ionic membrane	1 M NaClO ₄ in EC/PC	0.1	-	> 250 h	100
Na–Na	Graphene	1 M NaPF ₆ EC/DEC	0.5	0.5	200 h	102
		1 M NaPF ₆ EC/DEC	0.25	1	200 h	
		1 M NaPF ₆ EC/DEC	1	1	200 h	
		1 M NaPF ₆ EC/DEC	2	1	125 h	
		1 M NaPF ₆ EC/DEC	2	3	300 h	
		1 M NaPF ₆ EC/DEC	2	3	300 h	
		1 M NaPF ₆ EC/DEC	2	3	300 h	
Na–Na	Carbon paper	1 M NaClO ₄ in PC with 5%FEC	1	1	200 cycles	103
		1 M NaCF ₃ SO ₃ in DGME	0.5	1	250 cycles	
		1 M NaCF ₃ SO ₃ in DGME	5	1	1200 cycles	

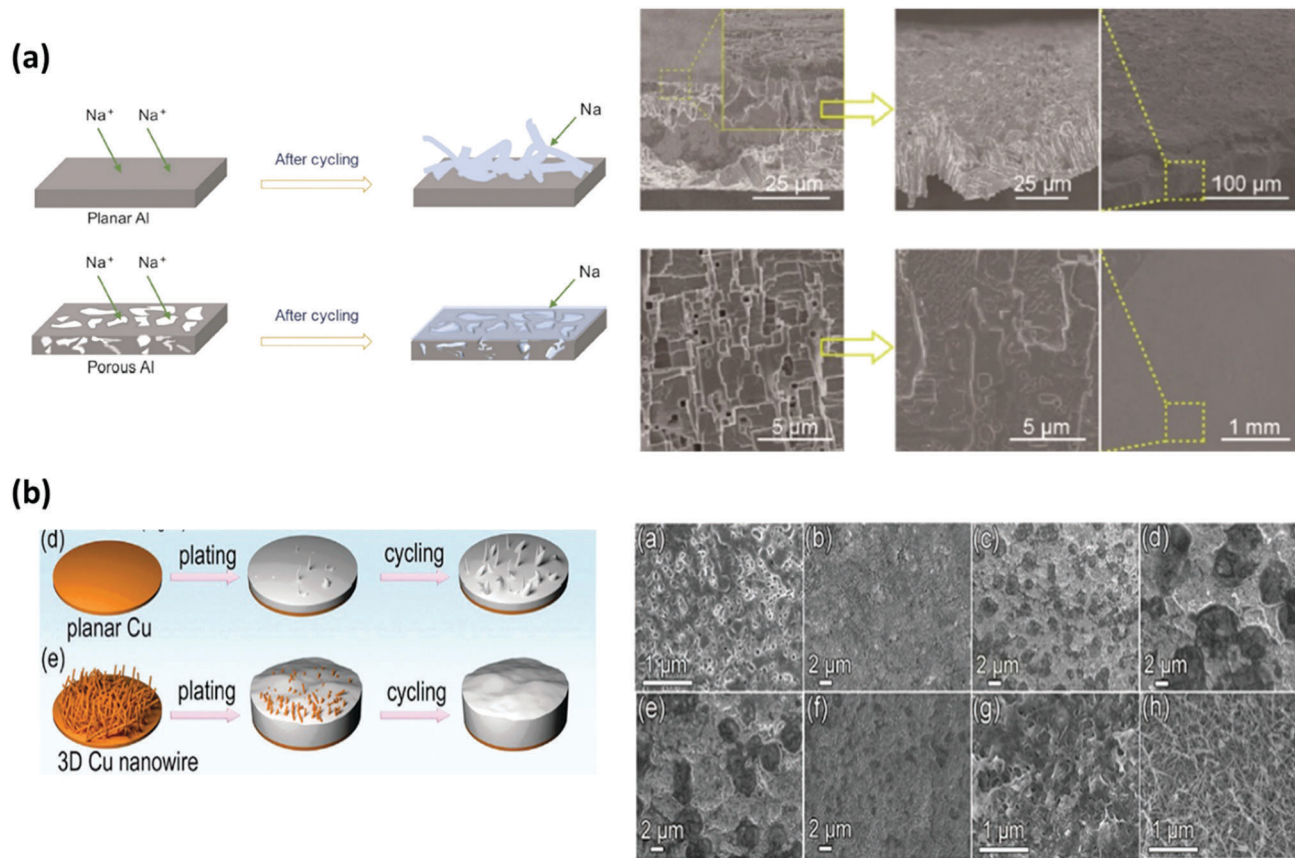


Fig. 6 (a) Schematic of Na deposition on planar and porous Al foils; SEM images of porous Al foils before and after plating/stripping cycling.¹⁰⁶ Reproduced with permission from American Chemical Society. (b) Schematic illustrations of Na-plating models on different current collectors of Cu foil and 3D Cu nanowires; SEM images of 3D Cu nanowires after Na plating/stripping with different current densities and capacities.¹⁰⁷ Reproduced with permission from The Royal Society of Chemistry.

surface of the porous Al without any protuberance. As a result, the Na metal anodes can run for 1000 cycles with a low and stable voltage hysteresis and an average plating/stripping CE above 99.9% for over 1000 cycles.

Other kinds of nanostructured current collectors have been designed, including 3D Cu with nanowires, porous 3D Ni, carbon nano-template and 3D carbon fiber scaffolds.^{107–110} Lu and colleagues reported a facile hydrothermal route to transform commercial Cu foil into 3D Cu nanowires for use as current collector.¹⁰⁷ Fig. 6(a) shows the schematic illustrations of Na-plating models on different current collectors of planar Cu foil and 3D Cu nanowires. The as-prepared 3D Cu nanowires exhibited an average diameter of 40 nm, which can lead to a more effective electric field. As a result, the 3D Cu nanowires can accommodate a high areal capacity of 3 mA h cm⁻² with stable plating/stripping for over 100 cycles. Fig. 6(a) display the SEM images of the Na plating/stripping on 3D Cu nanowires at different capacities. When increasing the plating capacity to 4 mA h cm⁻², the deposited Na showed a nodule-like structure with round-shaped edges on the 3D Cu nanowires.

Generally, the energy barrier between Na and Cu (or Al) is relative high especially in the initial nucleation process, resulting in high over-potentials and non-uniform depositions.

In a recent work, macroporous catalytic carbon nanotemplates (MC-CNTs) composed of hierarchically interconnected carbon nanofibers were synthesized from microbe-derived cellulose *via* simple heating at temperatures from 800 to 2400 °C. Compared with Al foil, the MC-CNTs delivered lower initial over-potentials, which can be attributed to the lower energy barrier. The MC-CNT fabricated at high temperature (2400 °C) maintained better cycling behavior with a CE of 99.9% over 1000 cycles, and in contrast, the MC-CNT fabricated at 800 °C shows a limited cycling stability (~200 cycles). It is believed that degradation of the graphitic structure for MC-CNT-2400 is significantly retarded in the repetitive cycles, which can cause a remarkable improvement in cycling performances. Recently, another impressive work has been reported by Tang *et al.*¹¹¹ where they introduced a “sodiophilic” layer of Au–Na alloy on the Cu substrate to significantly reduce the energy barriers and over-potential during the nucleation process. From their results, an average CE of 99.8% can be maintained at a high current density of 2 mA cm⁻² for 300 cycles.

In this section, we summarize the reported research on the design of nanostructured current collector for NMBs, particularly for anode-free NMBs (Table 3). Several works have demonstrated the use of 3D metal and carbon substrates as

Table 3 Summary of the reported literature on nanostructured current collectors for Na metal anodes

Na cells	Current collector	Electrolyte	Current density (mA cm ⁻²)	Capacity (mA h cm ⁻²)	CE/life time	Ref.
Na-Al	Al/carbon	1 M NaPF ₆ in DEGDME	0.5	0.25	99.8%/(1000 cycles)	105
Na-Al	Porous Al foil	1 M NaPF ₆ in DEGDME	0.5	0.25	99.9%/(1000 cycles)	106
		1 M NaPF ₆ in DEGDME	1	0.5	99.8%/(1000 cycles)	
Na-Cu	3D Cu nanowire	1 M NaPF ₆ in DEGDME	0.5	0.5	99%/(200 cycles)	107
Na-Ni	Porous 3D Ni	1 M NaPF ₆ in DEGDME	1	0.5	99.5%/(220 cycles)	108
			1	1	> 95%/(110 cycles)	
			1	2	> 95%/(50 cycles)	
Na-C	Macroporous catalytic carbon nanotemplates	1 M NaPF ₆ in DEGDME	1	0.5	99.8%/(1000 cycles)	109
Na-C	Carbon fibers	1 M NaCF ₃ SO ₃ in diglyme	1	1	99.5%/(100 cycles)	110
Na-Cu	Au on Cu	1 M NaCF ₃ SO ₃ in diglyme	2	1	99.8%/(300 cycles)	111

current collectors to achieve stable performances with high CE of 99% and superior long life times of over 1000 cycles. However, some challenges still remain: (1) the electrolyte systems used in these studies are among the most stable electrolytes (NaPF₆ in DEGDME), as discussed in 3.1. However, there is no report focusing on the dendrite-free Na deposition and high CE of current collector in carbonate-based electrolyte, which is more popular for cells coupled with insertion-type Na cathodes. (2) The capacities are relatively low (< 1 mA h cm⁻²), which is insufficient for practical applications that require high capacity. (3) Although carbon materials have been used to decrease the energy barriers of Al, large over-potentials are still present under high current density. Thus, there is still room for improvement with respect to the performances *via* modifying the current collector with specific materials which have low energy barriers during Na nucleation, such as gold.

4.2 Nanostructured hosts for Na metal

As discussed above, another serious issue for metallic Na is the relatively infinite volume change, which has only recently begun to be addressed. To overcome this problem, molten Li is introduced into the gaps of nanostructured host materials.⁵⁰ Different from the 3D current collector, this strategy is very important for the application of stable Na metal anodes in RT Na-S and Na-O₂ batteries, in which the cathode materials lack prestored Na. Nanostructured carbon materials are the most popular candidate as host due to their low cost, ease of fabrication and stable chemical properties. Luo *et al.* used reduced graphene oxide (rGO) as a host to form a processable and moldable composite Na metal anode, as shown in Fig. 7(a).¹¹² Interestingly, it was observed that by controlling the thicknesses of the densely stacked graphene oxide (GO) film, the thicknesses of the Na@rGO can be easily determined, which was found to be 20 times that of the GO films (Fig. 7(a)). Meanwhile, the shapes and structures of the Na@rGO can be assembled into 1D fibers, 3D monoliths or other 2D shapes by changing the GO precursor. The composites with only 4.5% GO had greatly enhanced mechanical properties, such as hardness, strength, and stability against environmental corrosion compared to pure Na. The as-prepared Na@rGO composite electrodes showed enhanced electrochemical plating/stripping

performances in a series of electrolytes, including NaPF₆ in diglyme, NaCF₃SO₃ in diglyme and NaClO₄ in EC/PC. The r-GO sheets in the Na@r-GO composite could flatten the surface, leading to a more evenly distributed Na⁺ flux, further enhancement of the electrochemical performances and suppressed dendrite growth.¹¹² Moreover, wood-derived carbon materials with channels have also been reported by Hu and colleagues as a 3D host for Na metal.¹¹³ Fig. 7(b) illustrates the fabrication of the Na-wood composite electrode with the thermal infusion process of molten Na. After melt infusion of Na, the channels of carbonized wood were almost completely filled, as observed by SEM. The electrochemical performances of symmetric cells using Na-wood electrodes and bare Na electrode under different capacity limits are shown in Fig. 7(b). The Na-wood electrode displayed very stable cycling performance with more than 250 cycles under both testing conditions while the bare Na metal can only run for less than 90 cycles and 50 cycles, respectively. The improved performances can be attributed to the porous channels of the wood-derived carbon, which provide a high-surface-area conductive host that can greatly decrease the effective current density and ensure uniform Na nucleation. In our recent paper, we demonstrated the rational design of a carbon paper (CP) with N-doped carbon nanotubes (NCNTs) as a 3D host to obtain Na@CP-NCNTs composites electrodes for NMBs.¹¹⁴ The schematic diagram of the fabrication procedure of Na@CP-NCNTs composites is shown in Fig. 7(c). Interestingly, without NCNTs, the pristine CP was found to be “Na-phobic” and displayed a large contact angle between the substrate and molten Na. However, after functionalizing the CP with NCNTs, the contact angle between Na and CP-NCNTs was effectively reduced and Na was found to instantaneously diffuse into the 3D CP-NCNTs. These results demonstrated that NCNTs possess the ability to change the Na wettability properties of CP. We first proposed this phenomenon as “from Na-phobic into Na-philic”. As shown in Fig. 7(c), the Na@CP-NCNTs composite electrode exhibited more stable electrochemical performances compared to bare Na foil at high current density of 3 mA cm⁻² and even 5 mA cm⁻². Moreover, the Na@CP-NCNTs composites maintained a stable cycling performance at a high current density of 5 mA cm⁻² with a high capacity limit of 3 mA h cm⁻², which is promising for the practical application of LMBs.

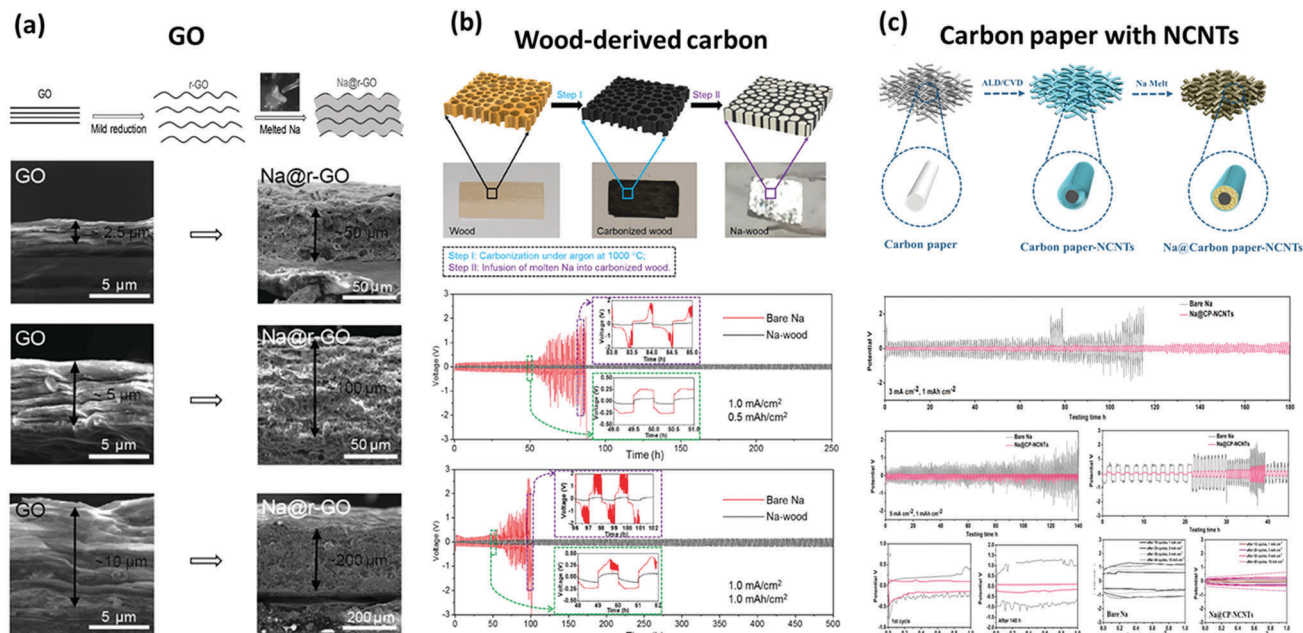


Fig. 7 (a) Schematic representation of the preparation and molten processes of Na@r-GO composites.¹¹² Reproduced with permission from John Wiley and Sons. (b) Encapsulation of metallic Na into carbonized wood by a spontaneous and instantaneous infusion and the electrochemical performances.¹¹³ Reproduced with permission from American Chemical Society. (c) Schematic diagram of the fabrication procedure of Na@CP-NCNTs and the electrochemical performances.¹¹⁴ Reproduced with permission from John Wiley and Sons.

Table 4 Summary of the reported literature on nanostructured hosts for Na metal anodes

Na cells	Host materials	Electrolyte	Current density (mA cm^{-2})	Capacity (mA h cm^{-2})	CE/life time	Ref.
Na-Na	RGO-Na	1 M NaClO ₄ in EC/PC	0.25	0.0625	300	112
	RGO-Na	1 M NaClO ₄ in EC/PC	0.5	0.125	60 h	
	RGO-Na	1 M NaPF ₆ in DEGDME	1	1	600 h	
		1 M NaCF ₃ SO ₃ in DEGDME	0.25	0.05	300 h	
		1 M NaCF ₃ SO ₃ in DEGDME	3	3	300 h	
Na-Na	Wood-carbon-Na	1 M NaClO ₄ in EC/DEC	0.5	0.25	250 h	113
			1	1	500 h	
			1	0.5	250 h	
Na-Na	Na@CP-NCNTs	1 M NaPF ₆ in EC/PC	1	1	350 h	114
			3	1	180 h	
			5	3	90 h	

Herein, we mainly focus on the progress of nanostructured hosts for Na metal anodes (Table 4), which is still in its infancy. Only a few studies have been reported using carbon materials for the thermal infusion process. Currently, more efforts should be put forward for both the surface chemistry involved in the thermal infusion process and achieving excellent performances with high reversible capacity.

5. Application of Na anodes in NMBs

In the previous section, we mainly discuss the different strategies to stabilize the Na metal anode. However, most of the studies focus on the electrochemical plating/stripping behaviours in symmetric cells or half cells. In this section, we will summarize the recent works using Na metal electrodes and their practical application in different NMB systems, including Na-CO₂, Na-O₂ and all-solid-state batteries.

5.1 Na-O₂ and Na-CO₂ batteries

As previously discussed, Na-O₂ batteries have attracted increasing attention as an alternative to LIBs due to their high theoretical energy density. Furthermore, Na-O₂ batteries possess the advantage of high energy efficiency due to lower charging overpotential compared to the Li-O₂ system. The improved energy efficiency can be attributed to the reversible electrochemistry of the oxygen/superoxide (O₂/O₂⁻) redox pair (compared to the semi-irreversible oxygen/peroxide (O₂/O₂²⁻) redox pair in Li-O₂ batteries). Most studies in this field are concentrated on the fundamental understanding of the discharge products, discharge/charge mechanism, cathode design and choice of catalyst.^{34,115,116} However, the O₂/O₂⁻ generated from the cathode may migrate towards the separator and metallic Na because of concentration gradients in the electrolyte. On one hand, the migrated intermediates may precipitate on the non-conductive separator, lowering the CEs of the batteries. On another hand,

both O_2/O_2^- will reaction with Na metal, resulting in an insulating oxide layer on the Na surface which will block the Na ion transport from the surface to bulk Na. Meanwhile, the Na dendrite growth is another common issue for the Na metal anode, even in Na- O_2 batteries. Furthermore, the Na dendrite growth and O_2 corrosion have been identified in real Na- O_2 cells as one of the most serious issues and limitation on the life time of the batteries.^{54,55,117} Bi *et al.* also showed the dendrite formation in Na- O_2 batteries in their paper.¹¹⁸ Based on the cell performances, the cycling life of the Na- O_2 batteries using DEM and diglyme as electrolyte fluctuated between 6 cycles to 12 cycles with voltage fluctuations during the charging process, as shown in Fig. 8(a). After disassembling the failed cells, spots were observed at the surface of glass fibre facing the metal anode, an indication that Na dendrites caused the shorting of the batteries. From the SEM images in Fig. 8(a), it was also verified that the Na metal had grown across more than 80% of the thickness of the separator in just a few cycles. As a potential solution, a Na ion selective membrane was employed between two GF separators to prevent dendrite penetration. The Nafion

membranes exhibited good mechanical strength and an ionic conductivity of $2.56 \times 10^{-5} \text{ S cm}^{-1}$ at RT. The results showed that the incorporation of the Nafion- Na^+ membranes greatly improves the cyclability of Na- O_2 batteries in both DME and diglyme-based electrolytes. Another group further extended this idea as an “interlayer” for suppressing the Na dendrite formation in Na- O_2 batteries.¹¹⁹ They studied several types of polymer films, including fibrillar polyvinylidene fluoride (f-PVDF), compact PVDF (c-PVDF), PVDF with through pores (p-PVDF), polyethylene oxide (PEO), and conventional polytetrafluoroethylene (PTFE). The cycling stability and rate performances of the Na- O_2 batteries using different interlayers are shown in Fig. 8(c), in which the f-PVDF is superior to the other tested polymers. It was believed that the performance stems from f-PVDF's uniform fiber structure for Na^+ distribution and high uptake of electrolyte for fine electrode-electrolyte contact, stable physical and chemical properties against the robust metal-air conditions, and strong affinity with electrolyte for improved ion conductivity.¹¹⁹ As an alternative to the introduction of an interlayer between Na and separator, Liang *et al.* demonstrated

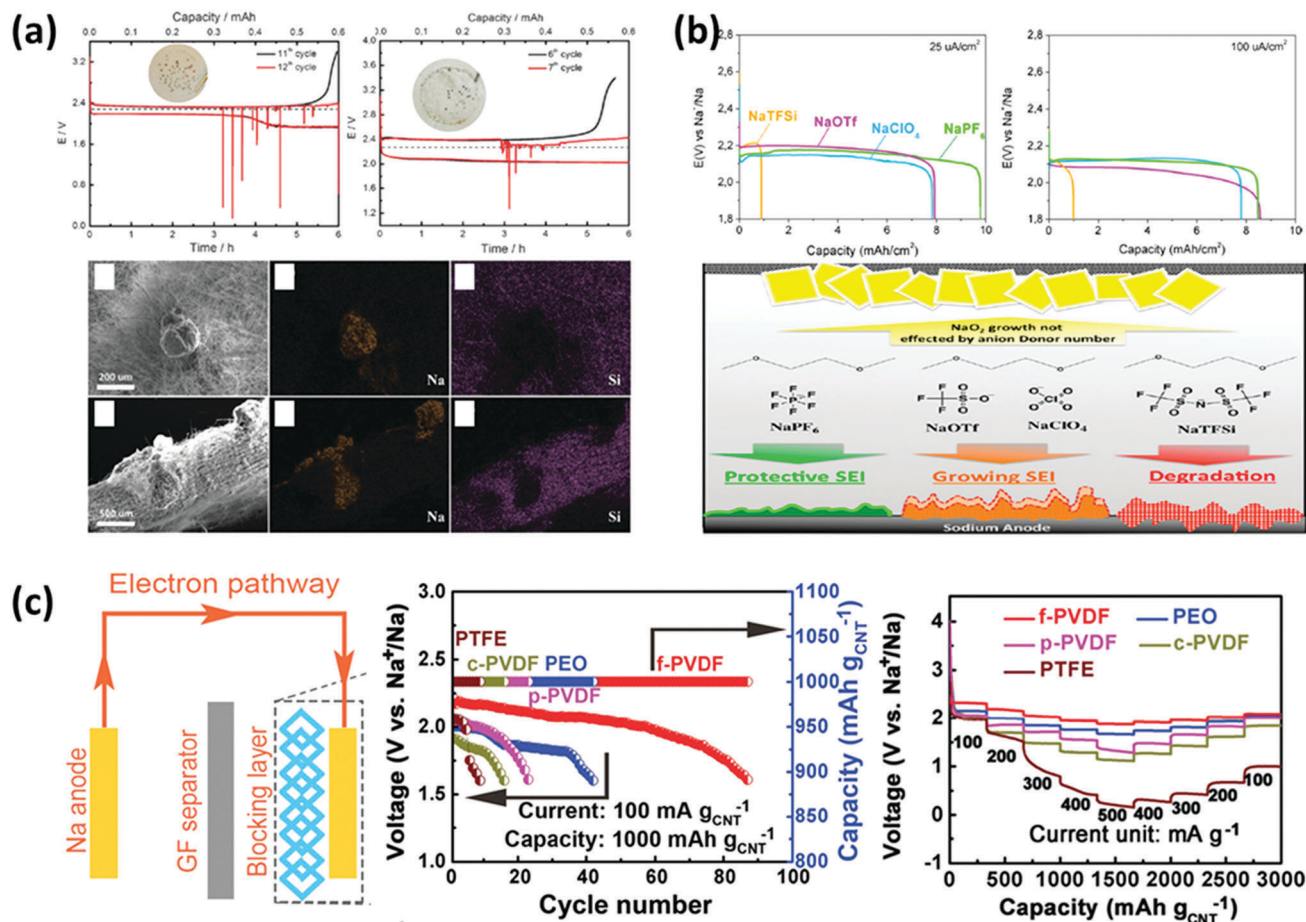


Fig. 8 Na metal anode in Na- O_2 batteries: (a) discharge/charge profiles of a Na- O_2 battery for the last two cycles in DME and diglyme; SEM and EDS mapping images the top-view and cross-section of the Na dendrite in GF separators.¹¹⁸ Reproduced with permission from The Royal Society of Chemistry. (b) Na- O_2 cell discharges at current densities of 25 $\mu\text{A cm}^{-2}$ as well as 100 $\mu\text{A cm}^{-2}$ with different electrolytes; illustration of sodium SEI formation mechanism and its composition in different DME electrolytes.¹²¹ Reproduced with permission from American Chemical Society. (c) Schematics of the symmetrical battery design using interlayer for Na metal anode; the rate capability, voltage of the terminal discharge versus the cycle number curves of Na- O_2 batteries with the five blocking interlayers.¹¹⁹ Reproduced with permission from John Wiley and Sons.

a new trilayer separator for Na–O₂ batteries.¹²⁰ A middle layer of TiO₂ nanoparticles were synthesized within the separators to form a sandwich structure. Their results show that the cycling life of Na–O₂ batteries can be enhanced from 82 cycles to 137 cycles using the TiO₂ sandwich separator, in which the TiO₂ nanoparticles can react with Na metal and slow down the Na dendrite growth during cycling.

As previously discussed, the electrolyte components including the solvent and salt have a major influence on the Na deposition behaviour. Lutz *et al.* discovered that the sodium salt anion plays an important role on the performances of real Na–O₂ batteries.¹²¹ Fig. 8(b) show the Na–O₂ cell discharges with different electrolytes and an illustration of suggested SEI formation mechanism in the different DME electrolytes. Similarly, NaF formation in the SEI seemed to be a crucial component for improved stability of the Na anode in the Na–O₂ batteries. Subsequently, Zhou and colleagues presented a durable protection film containing NaF on the surface of the Na anode to achieve stable Na–O₂ batteries.¹²² The Na anode with a durable protection film was prepared by discharging and charging a symmetric cell using an ether-based electrolyte (NaCF₃SO₃ in tetraglyme with 2%FEC). The large amount of NaF in the film endows the metallic Na anode with superior merits to effectively limit the O₂ crossover and electrolyte related side reactions, and further suppresses the formation of by-products. Moreover, the formation of Na dendrites can be avoided and long term cycling stability could be achieved without short circuits. In addition, nanostructured porous Al foil and 3D Na@rGO have been investigated in Na–O₂ batteries as a proof of concept by Luo's group.^{106,112}

In addition to Na–O₂ batteries, Na–CO₂ batteries using greenhouse gas CO₂ are also interesting topic as a new type of battery system. The system still poses safety risks from leakage of liquid electrolyte and instability of the metallic Na anode. Chen's group reported the quasi-solid-state Na–CO₂ cells with polymer electrolyte and reduced graphene oxide (rGO) Na anodes.¹²³ In their study, the rGO-Na anode presented fast and non-dendritic Na⁺ plating/stripping behavior. The rationally designed Na–CO₂ batteries can be successfully cycled in a wide CO₂ partial pressure window with a long life time of over 400 cycles.

Briefly, we have summarized the recent works focusing on the metallic Na anode in Na–O₂ and Na–CO₂ batteries. Differing from symmetric cells and half cells, the metallic Na not only suffer from the dendritic Na growth, but also possesses other issues such as O₂/O₂[–] cross over and by-product corrosion. To address the challenges associated with O₂/O₂[–] crossover, approaches such as the introduction of conductive interlayers on the Na metal anode can allow side reactions to occur on the interlayer rather than the surface of Na metal. In this case, the surface of Na will not be corroded and the transport of Na⁺ will not be blocked. In addition, the exploitation of highly stable protective layers against O₂/O₂[–] is urgently required for use in Na–O₂ batteries systems, and is also expected to further stabilize the SEI formation and reduce Na dendrite growth. Lastly, the air electrode (cathode) design should be optimized to

minimize the O₂/O₂[–] crossover issue. Thus, the use of metallic Na in practical Na–O₂ and Na–CO₂ batteries will be more challenging, in which additional factors need to be taken into consideration when designing the Na metal electrodes.

5.2 RT Na–S batteries

High temperature Na–S batteries have been previously developed and operate at 300 °C. In this system, both electrodes including the S cathode and Na anode are in a molten state, resulting in low energy efficiency along with corrosion and safety hazards. To overcome these issues, RT Na–S batteries have been firstly demonstrated in 2006.²⁷ The RT Na–S batteries follow similar working principles with Li–S batteries and share many of the challenges faced by the similar battery system. The main challenges include the insulating nature of the Na₂S discharge products; dissolution of polysulfide species; shuttle effects of polysulfides and dendrite formation on Na metal.^{26,27,124} The efforts in this field have been primarily focused on the development of functional nanocomposites, utilizing efficient electrolytes, and constructing novel cell configurations to obtain high performance RT Na–S batteries.²⁷

However, it also has been noticed that the surface degradation of the Na anode is a major concern for the capacity degradation of the RT Na–S batteries.¹²⁵ From the studies by Manthiram's group, it was shown that the surface of the Na anode became severely rough after cycling (100 cycles) even with the designed functional separator.¹²⁵ Therefore, besides the suppression of the polysulfide shuttling effect, protection of the metallic Na anode would be another important research area to achieve long cycle life RT Na–S batteries.¹²⁶

5.3 All-solid-state Na metal batteries

SSNMBs are a promising choice for next-generation energy storage devices beyond LIBs because of their enhanced safety and ability to achieve high-energy and high-power densities by replacing the liquid electrolytes with SSEs.^{38,127,128} From our discussion above, the SEI layer caused by the reactions between Na and liquid electrolyte is the key factor that determines the life time of the Na metal anode. This phenomenon has also been recently proven by Goodenough and colleagues through the use of TOF-SIMS, as shown in Fig. 9(a).¹²⁹ However, when they replace the liquid electrolyte with a NASICON Na₃Zr₂Si₂PO₁₂ electrolyte, the side reactions are effectively limited, as revealed by the formation of a passivating interface with a significantly reduced thickness on the surface of the metallic Na anode. The battery performances have also been significantly enhanced in solid-state batteries using the a Na₂MnFe(CN)₆ cathode.

Despite the benefits of SSNMBs, it should be noted that the interface between SSEs and Na metal anode can still be an issue. Some types of electrolyte may react with Na metal to form unstable interfaces and cause degradation of the SSEs. Janek's group explored the stability and viability between Na metal and two kind of electrolytes of Na₃PS₄ and Na-β''-Al₂O₃.¹³⁰ As expected, Na-β''-Al₂O₃ is stable against sodium, whereas Na₃PS₄ decomposes with an overall resistance that increases with time. They also proposed three possible interphases between

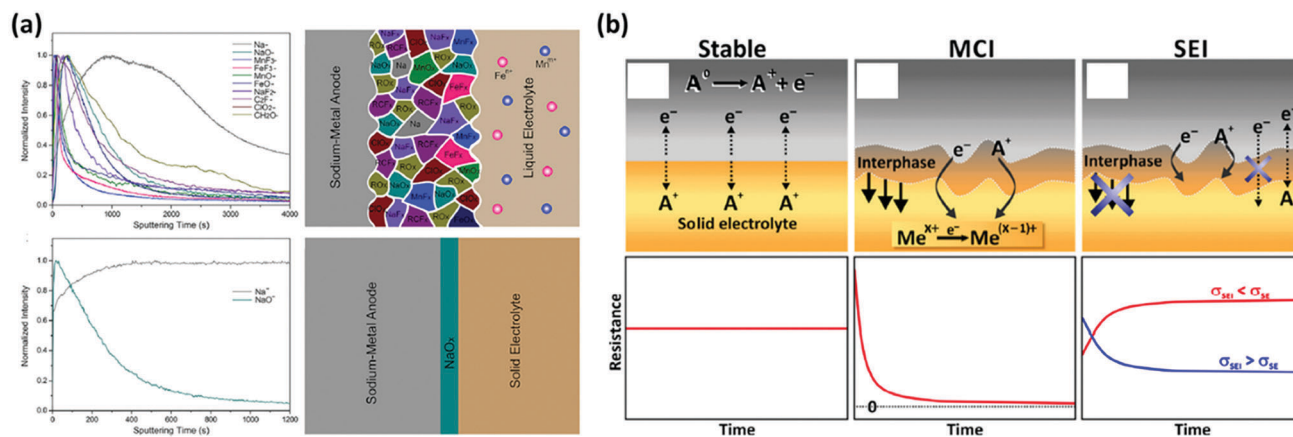


Fig. 9 Na metal anode in solid-state batteries: (a) distribution of different chemical compositions on the surface of the sodium-metal anodes after the cycling tests in both liquid cell and SSBs.¹²⁹ Reproduced with permission from Elsevier. (b) Illustrations of three possible interphases between electrolyte and electrode materials: a stable interface (stable), a mixed-conducting interphase (MCI), and the solid electrolyte interphase (SEI) with the corresponding time-dependent resistance is shown below.¹³⁰ Reproduced with permission from American Chemical Society.

electrolyte and electrode materials, including the stable interface (stable), a mixed-conducting interphase (MCI), and the solid electrolyte interphase (SEI) (Fig. 9(b)). Recently, Meng's group also studied the interface between the sodium anode and sulfide-based solid electrolytes, including Na_3SbS_4 , Na_3PS_4 , and Cl-doped Na_3PS_4 in SSNMBs.¹³¹ From their results, solid electrolyte interphases between Na_3SbS_4 and Na, as well as Na_3PS_4 and Na, are predicted computationally to be composed of Na_2S and Na_3Sb , Na_2S and Na_3P , respectively, due to the chemical reactions between SSEs and Na metal. Interestingly, Cl-doped Na_3PS_4 shows the presence of an additional compound of NaCl at the interface, which is found to mitigate the decomposition of Na_3PS_4 . From their results, new insight and an approach to reduce the chemical reactions and improve the interface stability between SSEs and Na metal has been developed by the doping of other elements.

To engineer the interface between SSEs and Na metal anode, Goodenough and colleagues designed two different approaches to enhance the compatibility of NASICON $\text{Na}_3\text{Zr}_2\text{Si}_2\text{PO}_{12}$ and Na metal.¹³² Firstly, it was found that the molten Na cannot wet the surface of NASICON SSEs under low temperature (175 °C), leading to a high resistance between Na metal and SSEs. Promisingly, when increasing the temperature up to 380 °C for 30 min, the wettability between Na metal and SSEs significantly improved, resulting in reduced resistance. Another strategy proposed in their paper was the use of a dry polymer as an interlayer between the SSEs and Na metal. This polymer interlayer can not only reduce the large interfacial resistance but also prevent dendrite formation. Excellent cycling performance and high CE SSNMBs were demonstrated with two strategies for good electrochemical stability and high Na deposition efficiency across a Na/SSE interface. Meanwhile, Ong *et al.* proposed different coating layers on Na metal to prevent the reactions between Na metal and sulfide SSEs based on the first-principles calculations, including Sc_2O_3 , SiO_2 , TiO_2 , ZrO_2 , and HfO_2 .¹³³ They explored these coatings and found that the $\text{Na}_2\text{Ti}_3\text{O}_7$ anode is predicted to be much more stable against a broad range of solid electrolytes compared with other metal oxides.

The development of SSNMBs is still in a very early stage. Significant efforts have been put forward to develop different types of SSEs with high ionic conductivity and chemical/electrochemical stability. However, when metallic Na is used as the anode, the interface between the SSEs and Na metal should be brought to the forefront. Forming a stable interface will be very important to obtaining long life SSNMBs. Surface modifications on Na or SSEs will be an effective approach to prevent these detrimental reactions. Unlike the solid-liquid interphase, the Na deposition behaviours will be determined not only by the surface chemistry of Na metal, but also by the properties of the SSEs. Thus, the Na dendrite growth along the grain boundaries in SSEs will be another potential issues and more experimental works will be needed to gain a fundamental understanding of the process. Lastly, the volume change of Na metal during plating/stripping may still exist in SSNMBs. Potential strategies such as using nanostructured Na metal electrodes are still promising avenues to alleviating this issue.

6. Conclusion

In summary, we have provided insight into the development and protection of Na metal anodes for NMBs, as shown in Fig. 10. Firstly, preliminary mechanisms have been proposed for Na dendrite growth. Particularly, the Na dendrites show weakened chemical, electrochemical and mechanical properties compared to their Li counterparts, and require stronger protection to inhibit dendrite formation. Meanwhile, the surface modification on Na metal is necessary due to corrosion of Na metal by the electrolyte in the absence of any electrochemical process, which differs from the Li metal electrode.

Secondly, different techniques have been used to study the composition and formation of Na dendrites and its SEI layers, including SEM, optical images, XPS, TOF-SIMS, and RBS. Impressively, various *in situ* techniques, such as *in situ* optical observation, *in situ* AFM, *in situ* NMR and *in situ* SEM/TEM,

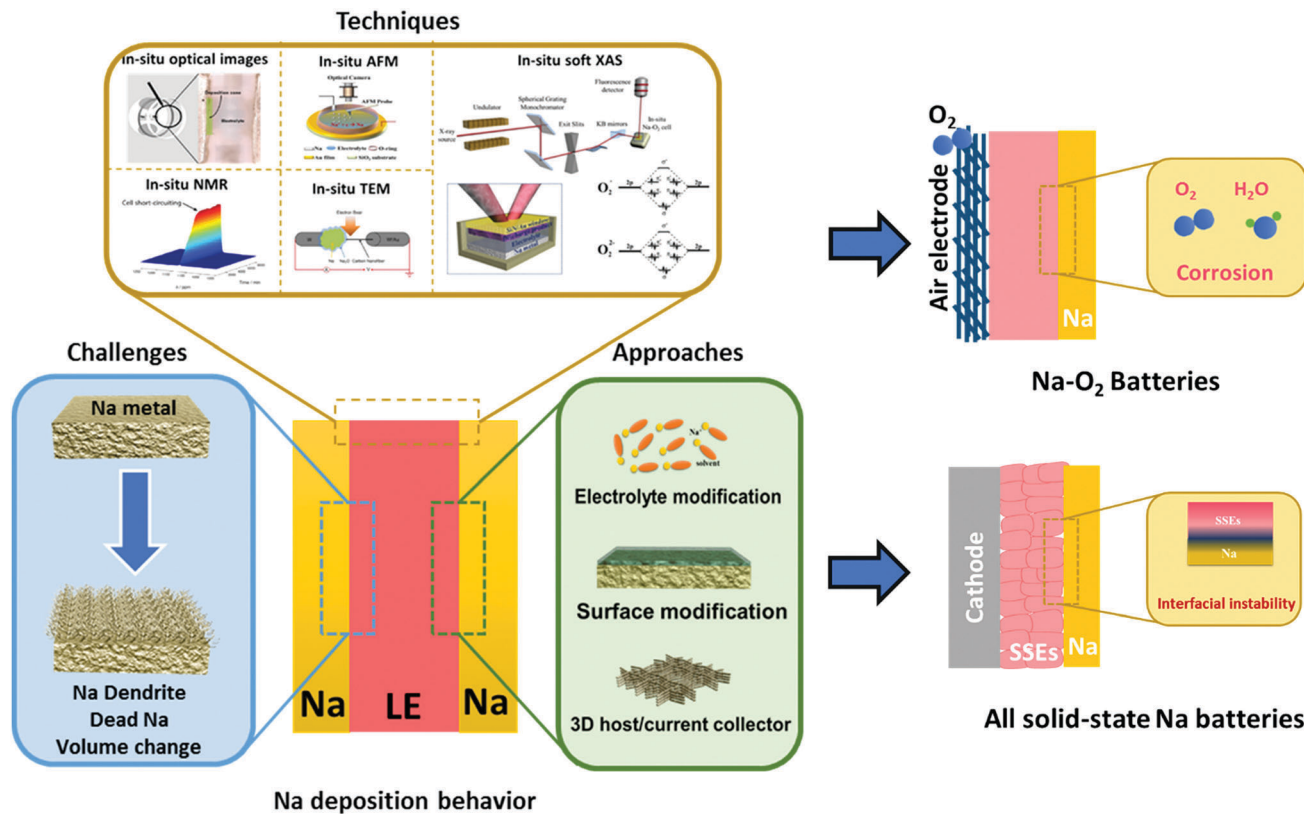


Fig. 10 Schematic diagram of the fundamental challenges of Na metal anodes and the protection methods used for their practical application.^{63–66,136} Reproduced with permission from American Chemical Society, The Royal Society of Chemistry and Elsevier.

have been demonstrated to provide new and more accurate methods of viewing the deposition behaviour of Na metal.

Thirdly, different strategies have been developed to reduce Na dendrite growth and enable long life Na metal anodes. (1) Electrolyte modifications. Since electrolytes play an important role during the SEI layer formation, a lot of studies have focused on the electrolyte modification. From previously reported comprehensive studies, the electrolytes consisting of NaPF₆ as a salt and glymes as solvent are the best choice, which can enable the formation of a uniform inorganic SEI layer consist of Na₂O and NaF which can inhibit dendrite growth. Furthermore, ultra-high salt concentrations or the introduction of “inert” diluents in the electrolyte have been shown to make remarkable influences on the suppression of Na dendrites and stabilization of the SEI layers. In addition, additives like FEC can also aid in the formation of NaF-containing SEI with improved CE and reduced dendrite growth. Moreover, novel electrolyte systems are still under exploration to further address the current issues in NMBs. (2) Surface modification. Three different methods of developing artificial SEI layers on Na metal anode have been identified, including the chemical/physical deposition method, the reaction method using Na as a reactant and the mechanical transfer method. Each of these methods show their own advantages and disadvantages, which are discussed in Section 3.2. (3) Nanostructured current collectors. 3D current collectors are used to dissipate the local current density and produce uniform Na⁺ flux for Na metal anode-free Na batteries. Different materials, including Al/carbon films, porous Al films,

3D Cu nanowires, 3D Ni, macroporous catalytic carbon nanotemplates and carbon fibers are reported to achieve very stable performances with high CE. (4) Nanostructured hosts. Rationally designed carbon materials, such as rGO, wood-derived carbon and carbon paper with carbon nanotube matrices, have been used as a host/matrix for the thermal infusion of molten Na. The 3D structure of Na metal composite electrodes exhibit suppressed dendrite growth, enhanced electrochemical performances, and minimized volume change during the plating/stripping process.

Lastly, the current progress of Na metal anodes in different NMBs, like Na–O₂, Na–CO₂ and SSNMBs, have been summarized. (1) In Na–O₂ batteries, the Na metal not only suffers from dendritic Na growth, but also has other issues such as O₂ cross over and by-products of corrosion. One of the most popular approaches to alleviate these issues is to introduce a functional “interlayer” and modify the surface of Na to block the O₂ cross over and reduce the dendrite growth. (2) The SSEs in SSNMBs can prevent the unstable SEI formation compared to liquid-based cells. However, the reactions between SSEs and Na have also been noticed as an issue. Thus, the interface stability between the SSEs/Na is the key to obtaining long life SSNMBs.

7. Perspective

Although there has been some progress related to the development of Na metal anodes, there are still significant challenges

to be overcome, particularly for the practical application of NMBs. Herein, we propose potential directions and perspectives for this field:

(1) Similarities and differences with Li metal anodes: Li metal anodes have been intensively studied over the past decades due to their high energy density and low electrochemical potential. Significant progress has been achieved towards the development of Li metal batteries (LMBs), including gains in the fundamental understanding of Li dendrite growth and the design of effective approaches for Li dendrite prevention. However, research on the Na metal anode in room temperature NMB systems is still in a state of infancy. Compared with the Li metal anode in LMBs, there is still significant room for further improvement of Na metal anodes: (i) longer lifespan. For Li metal anodes, the life time in Li–Li symmetric cells can reach thousands of hours with small increases of voltage polarization.⁵⁶ With the current status of Na metal anodes, the range for symmetric cell cycling is still in the hundreds of hours, which needs to be further improved to meet the demand of long lifespans. (ii) Large capacity and current density. Recently, large capacities (up to 10 mA h cm⁻²) and high current densities (up to 10 mA cm⁻²) have been achieved for high performances Li metal anodes.⁵⁶ However, the reported Na metal anodes are cycled with relatively lower capacities (<3 mA h cm⁻²) and current densities (<5 mA cm⁻²), which is far from the requirements of practical applications. In this case, research should be directed towards the development of strategies for high capacity and current density Na metal anodes. (iii) Better fundamental understanding of the Na deposition process. Unlike the systematic studies on Li metal anodes, few studies have focused on the fundamental understanding of the Na deposition process. Firstly, the Na deposition structures, including mossy and dendritic Na, should be better defined. Particularly, the relationship between Na deposition with other parameters, such as current density, capacity, temperature and pressure *etc.* should be further explored. Secondly, the nucleation process of Na is a fundamental aspect that is poorly understood, and more work should include studies on the nucleation locations and times. Thirdly, detailed information related to the SEI formation mechanism, structure, components, and regulation is still inadequate. (iv) Analytical and protective approaches from the field of Li metal batteries. Firstly, different analytical techniques used for the study of Li metal anodes, such as cryo-TEM and X-ray tomographic microscopy, are also promising to understand the SEI formation and dendrite growth of Na metal anodes. Secondly, ionically conductive SSEs as protective layers for Li metal anodes have been reported using different methods. The development of these types of protective layers on Na metal is expected to be another effective strategy to redistribute the Na⁺ flux on the surface and suppress Na dendrite growth. (v) SEI layer sensitivity. As discussed above, the Na metal, Na dendrite and the relevant SEI layers are more chemically and electrochemically sensitive to the electrolyte and external environments compared to their Li counterparts. It will be more challenging to address the issues of the Na metal anode compared to the problems associated with Li metal anodes.

(2) Advanced characterization techniques and methods: although different techniques have been applied to study the Na anode, a proper fundamental understanding of Na nucleation, dendrite growth, and chemical/electrochemical reactivity are still unclear, and require advanced techniques and characterization. Firstly, synchrotron radiation-related techniques will be excellent candidates for the study of the SEI layer on Na metal, especially with *in situ* capabilities. Synchrotron-based X-ray techniques, such X-ray absorption spectroscopy (XAS) and XPS, can act as strong tools for the understanding of SEI formation on the surface of Na metal. For example, high-energy XPS with tunable excitation photon energy can provide non-destructive depth profiling and chemical information not limited to the surface, which is attractive to study the surface and interfacial changes on Na metal. Moreover, X-ray tomographic microscopy, with spatial resolution on the micrometer scale, can be used for 2D and 3D investigations of the Na deposition process and the formation of dendritic structures. Furthermore, transmission X-ray microscopy is capable of probing the structural and chemical information of samples at the nanoscale (down to 20 nm) simultaneously, which can also be used to study Na dendrite growth and SEI composition. Secondly, due to the high reactivity of Na metal, cryo-based techniques are an ideal approach to obtaining the most authentic chemical information without any compositional changes of the Na dendrite or SEI layers. Thirdly, any one of these techniques is not enough to have a deep and comprehensive understanding on the surface and interface chemistry of the Na anode and its SEI layers, and the combination of different analysis technique in future research will be required.

(3) Engineering the SEI: since the SEI is the key factor for the stability of the Na metal anode, surface modifications with artificial SEI layers have become a promising direction. While several coatings have been explored, other approaches still need to be developed for Na⁺ conductive protective layers, in which sputtering is a good choice to deposit Na-SSEs as artificial SEI on Na metal. Secondly, polymer based thin films with ionic conductivity and high flexibility will be another promising strategy. Particularly, polymer coatings incorporating self-healing functionalities can reconstruct the surface cracks produced during cycling. Thirdly, ALD and MLD are still remarkable to address the issues for Na metal anode, especially with precisely controlled thicknesses. However, new ALD/MLD films need to be developed with improved Na⁺ conductivity, density, and flexibility. Lastly, the combination of different approaches to fabricate hybrid protective layer or composite artificial SEI layers is required, in which the different layers can serve their own functions to form a real and robust protection layer.

(4) Nanostructured Na: for NMBs, more than 10 micrometers of Na is ideal for the repeated plating/stripping process. The infinite volume change is still a restriction for long life NMBs. In this case, the rational design of host matrices is critically needed for practical NMBs. The host structure should possess chemical, electrochemical, and mechanical stability. Meanwhile, the weight and volume percentage of the matrix in the whole composites electrode should be limited in order to

maximize the energy density of the cell. Furthermore, although metallic Na is encapsulated in the matrix, the SEI layer will still be formed at the point of contact with the electrolyte. Thus, it would be a better idea to combine the strategies of nanostructured Na with artificial SEI to synergistically improve the stability and electrochemical performances of Na metal anodes.

(5) Different NMB systems: apart from the existing issues of Na dendrite growth, dead Na formation and infinite volume change, more serious challenges appear in different NMB systems. For example, the O₂ cross over and by-product corrosion is an obvious issue in Na–O₂ batteries. Furthermore, the interface stability between SSEs and Na metal is another uncertainty in terms of different types of SSEs. In this case, these other factors should be taken into consideration when designing metallic Na anodes for real NMBs.

(6) Practical applications: firstly, it should be pointed out that the high CE is very important for practical battery applications. A high CE of >99.9% after 1000 cycles at relatively high current density has not been reported yet. Secondly, it has become an emerging protocol to test the average CE values for Li metal anode.¹³⁴ Meanwhile, several parameters, such as the capacity for cycling, can affect the average Li-CE value.¹³⁵ In this case, the development of more accurate method and protocols on determining Na-CE is also urgently required to display the real CE during electrochemical plating/stripping. Thirdly, for the NMBs with different cathodes, the requirements of the areal capacity and thickness of Na metal are different. Thus, the design of Na metal anode should be tailored to the choice of cathode, electrolyte and NMB system.

In conclusion, it seems that the use of only a single approach is not enough to solve all the existing issues of Na metal anodes. Thus, multi-strategy approaches with specific aims will bring the metallic Na anode closer to reality. We believe that with continued efforts, the Na metal anode will act as the “Holy Grail” for the next-generation NMBs for large scale energy storage applications.

Conflicts of interest

There are no conflicts to declare.

Acknowledgements

This research was supported by the Natural Science and Engineering Research Council of Canada (NSERC), the Canada Research Chair Program (CRC), the Canada Foundation for Innovation (CFI), and the University of Western Ontario (UWO).

References

- J. Lu, Z. Chen, F. Pan, Y. Cui and K. Amine, *Electrochem. Energy Rev.*, 2018, **1**, 35–53.
- S.-J. Tan, X.-X. Zeng, Q. Ma, X.-W. Wu and Y.-G. Guo, *Electrochem. Energy Rev.*, 2018, **1**, 113–138.
- Y. Zhao, X. F. Li, B. Yan, D. B. Xiong, D. J. Li, S. Lawes and X. L. Sun, *Adv. Energy Mater.*, 2016, **6**, 152175.
- K. N. Wood, M. Noked and N. P. Dasgupta, *ACS Energy Lett.*, 2017, **2**, 664–672.
- S. Xin, Y. You, S. Wang, H.-C. Gao, Y.-X. Yin and Y.-G. Guo, *ACS Energy Lett.*, 2017, **2**, 1385–1394.
- S. Wei, S. Choudhury, Z. Tu, K. Zhang and L. A. Archer, *Acc. Chem. Res.*, 2018, **51**, 80–88.
- Z. P. Cano, D. Banham, S. Ye, A. Hintennach, J. Lu, M. Fowler and Z. Chen, *Nat. Energy*, 2018, **3**, 279–289.
- D. Kundu, E. Talaie, V. Duffort and L. F. Nazar, *Angew. Chem.*, 2015, **54**, 3431–3448.
- A. Ponrouch, D. Monti, A. Boschini, B. Steen, P. Johansson and M. R. Palacin, *J. Mater. Chem. A*, 2015, **3**, 22–42.
- W. Luo and L. Hu, *ACS Cent. Sci.*, 2015, **1**, 420–422.
- B. L. Ellis and L. F. Nazar, *Curr. Opin. Solid State Mater. Sci.*, 2012, **16**, 168–177.
- H. Pan, Y.-S. Hu and L. Chen, *Energy Environ. Sci.*, 2013, **6**, 2338.
- N. Yabuuchi, K. Kubota, M. Dahbi and S. Komaba, *Chem. Rev.*, 2014, **114**, 11636–11682.
- W. Luo, F. Shen, C. Bommier, H. Zhu, X. Ji and L. Hu, *Acc. Chem. Res.*, 2016, **49**, 231–240.
- A. Bauer, J. Song, S. Vail, W. Pan, J. Barker and Y. Lu, *Adv. Energy Mater.*, 2018, 1702869.
- D. Saurel, B. Orayech, B. Xiao, D. Carriazo, X. Li and T. Rojo, *Adv. Energy Mater.*, 2018, 1703268.
- H. Kim, H. Kim, Z. Ding, M. H. Lee, K. Lim, G. Yoon and K. Kang, *Adv. Energy Mater.*, 2016, **6**, 1600943.
- Y. Liang, W. H. Lai, Z. Miao and S. L. Chou, *Small*, 2018, **14**, 1702514.
- L. Wu, X. Hu, J. Qian, F. Pei, F. Wu, R. Mao, X. Ai, H. Yang and Y. Cao, *Energy Environ. Sci.*, 2014, **7**, 323–328.
- Y. Liu, N. Zhang, L. Jiao and J. Chen, *Adv. Mater.*, 2015, **27**, 6702–6707.
- Y. Liu, X. Liu, T. Wang, L.-Z. Fan and L. Jiao, *Sustainable Energy Fuels*, 2017, **1**, 986–1006.
- C. Bommier and X. Ji, *Small*, 2018, **14**, 1702514.
- J. Deng, W.-B. Luo, S.-L. Chou, H.-K. Liu and S.-X. Dou, *Adv. Energy Mater.*, 2018, **8**, 1701428.
- M. D. Slater, D. Kim, E. Lee and C. S. Johnson, *Adv. Funct. Mater.*, 2013, **23**, 947–958.
- J. Song, B. Xiao, Y. Lin, K. Xu and X. Li, *Adv. Energy Mater.*, 2018, 1703082.
- D. Kumar, S. K. Rajouria, S. B. Kuhar and D. K. Kanchan, *Solid State Ionics*, 2017, **312**, 8–16.
- Y.-X. Wang, B. Zhang, W. Lai, Y. Xu, S.-L. Chou, H.-K. Liu and S.-X. Dou, *Adv. Energy Mater.*, 2017, **7**, 1602829.
- H. Yadegari, M. Norouzi Banis, A. Lushington, Q. Sun, R. Li, T.-K. Sham and X. Sun, *Energy Environ. Sci.*, 2017, **10**, 286–295.
- H. Yadegari, Y. Li, M. N. Banis, X. Li, B. Wang, Q. Sun, R. Li, T.-K. Sham, X. Cui and X. Sun, *Energy Environ. Sci.*, 2014, **7**, 3747–3757.
- Z. E. Reeve, C. J. Franko, K. J. Harris, H. Yadegari, X. Sun and G. R. Goward, *J. Am. Chem. Soc.*, 2017, **139**, 595–598.

- 31 S. Zhang, Z. Wen, J. Jin, T. Zhang, J. Yang and C. Chen, *J. Mater. Chem. A*, 2016, **4**, 7238–7244.
- 32 C. L. Bender, P. Hartmann, M. Vračar, P. Adelhelm and J. Janek, *Adv. Energy Mater.*, 2014, **4**, 1301863.
- 33 N. Ortiz-Vitoriano, T. P. Batcho, D. G. Kwabi, B. Han, N. Pour, K. P. Yao, C. V. Thompson and Y. Shao-Horn, *J. Phys. Lett.*, 2015, **6**, 2636–2643.
- 34 C. Xia, R. Black, R. Fernandes, B. Adams and L. F. Nazar, *Nat. Chem.*, 2015, **7**, 496–501.
- 35 S. Y. Sayed, K. P. Yao, D. G. Kwabi, T. P. Batcho, C. V. Amanchukwu, S. Feng, C. V. Thompson and Y. Shao-Horn, *Chem. Commun.*, 2016, **52**, 9691–9694.
- 36 C. Xia, R. Fernandes, F. H. Cho, N. Sudhakar, B. Buonacorsi, S. Walker, M. Xu, J. Baugh and L. F. Nazar, *J. Am. Chem. Soc.*, 2016, **138**, 11219–11226.
- 37 H. Yadegari, Q. Sun and X. Sun, *Adv. Mater.*, 2016, **28**, 7065–7093.
- 38 C. Zhao, L. Liu, X. Qi, Y. Lu, F. Wu, J. Zhao, Y. Yu, Y.-S. Hu and L. Chen, *Adv. Energy Mater.*, 2018, 1703012.
- 39 J.-J. Kim, K. Yoon, I. Park and K. Kang, *Small Methods*, 2017, **1**, 1700219.
- 40 W. D. Richards, T. Tsujimura, L. J. Miara, Y. Wang, J. C. Kim, S. P. Ong, I. Uechi, N. Suzuki and G. Ceder, *Nat. Commun.*, 2016, **7**, 11009.
- 41 A. Inoishi, T. Omuta, E. Kobayashi, A. Kitajou and S. Okada, *Adv. Mater. Interfaces*, 2017, **4**, 1600942.
- 42 Q. Ma, J. Liu, X. Qi, X. Rong, Y. Shao, W. Feng, J. Nie, Y.-S. Hu, H. Li, X. Huang, L. Chen and Z. Zhou, *J. Mater. Chem. A*, 2017, **5**, 7738–7743.
- 43 J. Mindemark, R. Mogensen, M. J. Smith, M. M. Silva and D. Brandell, *Electrochem. Commun.*, 2017, **77**, 58–61.
- 44 S.-i. Nishimura, N. Tanibata, A. Hayashi, M. Tatsumisago and A. Yamada, *J. Mater. Chem. A*, 2017, **5**, 25025–25030.
- 45 F. Lalère, J. B. Leriche, M. Courty, S. Boulineau, V. Viallet, C. Masquelier and V. Seznec, *J. Power Sources*, 2014, **247**, 975–980.
- 46 Z. Yu, S. L. Shang, J. H. Seo, D. Wang, X. Luo, Q. Huang, S. Chen, J. Lu, X. Li, Z. K. Liu and D. Wang, *Adv. Mater.*, 2017, **29**, 1605561.
- 47 T.-S. Wang, Y. Liu, Y.-X. Lu, Y.-S. Hu and L.-Z. Fan, *Energy Storage Mater.*, 2018, **15**, 274–281.
- 48 Y. Guo, H. Li and T. Zhai, *Adv. Mater.*, 2017, **29**, 1700007.
- 49 Y. Zhao, Q. Sun, X. Li, C. Wang, Y. Sun, K. R. Adair, R. Li and X. Sun, *Nano Energy*, 2018, **43**, 368–375.
- 50 D. Lin, Y. Liu and Y. Cui, *Nat. Nanotechnol.*, 2017, **12**, 194–206.
- 51 J. T. Vaughey, G. Liu and J.-G. Zhang, *MRS Bull.*, 2014, **39**, 429–435.
- 52 H. Yang, C. Guo, A. Naveed, J. Lei, J. Yang, Y. Nuli and J. Wang, *Energy Storage Mater.*, 2018, **14**, 199–211.
- 53 A. Boschini, M. E. Abdelhamid and P. Johansson, *ChemElectroChem*, 2017, **4**, 2717–2721.
- 54 P. Hartmann, M. Heinemann, C. L. Bender, K. Graf, R.-P. Baumann, P. Adelhelm, C. Heiliger and J. Janek, *J. Phys. Chem. C*, 2015, **119**, 22778–22786.
- 55 N. Zhao, C. Li and X. Guo, *Phys. Chem. Chem. Phys.*, 2014, **16**, 15646–15652.
- 56 X. B. Cheng, R. Zhang, C. Z. Zhao and Q. Zhang, *Chem. Rev.*, 2017, **117**, 10403–10473.
- 57 D. Wang, W. Zhang, W. Zheng, X. Cui, T. Rojo and Q. Zhang, *Adv. Sci.*, 2017, **4**, 1600168.
- 58 J. Lang, L. Qi, Y. Luo and H. Wu, *Energy Storage Mater.*, 2017, **7**, 115–129.
- 59 K. Zhang, G.-H. Lee, M. Park, W. Li and Y.-M. Kang, *Adv. Energy Mater.*, 2016, **6**, 1600811.
- 60 X. B. Cheng, R. Zhang, C. Z. Zhao, F. Wei, J. G. Zhang and Q. Zhang, *Adv. Sci.*, 2016, **3**, 1500213.
- 61 Y.-S. Hong, N. Li, H. Chen, P. Wang, W.-L. Song and D. Fang, *Energy Storage Mater.*, 2018, **11**, 118–126.
- 62 W. Xu, J. Wang, F. Ding, X. Chen, E. Nasybulin, Y. Zhang and J.-G. Zhang, *Energy Environ. Sci.*, 2014, **7**, 513–537.
- 63 R. Rodriguez, K. E. Loeffler, S. S. Nathan, J. K. Sheavly, A. Dolocan, A. Heller and C. B. Mullins, *ACS Energy Lett.*, 2017, **2**, 2051–2057.
- 64 M. Han, C. Zhu, T. Ma, Z. Pan, Z. Tao and J. Chen, *Chem. Commun.*, 2018, **54**, 2381–2384.
- 65 P. M. Bayley, N. M. Trease and C. P. Grey, *J. Am. Chem. Soc.*, 2016, **138**, 1955–1961.
- 66 X. Li, L. Zhao, P. Li, Q. Zhang and M.-S. Wang, *Nano Energy*, 2017, **42**, 122–128.
- 67 H. Kondou, J. Kim and H. Watanabe, *Electrochemistry*, 2017, **85**, 647–649.
- 68 M. Gauthier, T. J. Carney, A. Grimaud, L. Giordano, N. Pour, H. H. Chang, D. P. Fenning, S. F. Lux, O. Paschos, C. Bauer, F. Maglia, S. Lupart, P. Lamp and Y. Shao-Horn, *J. Phys. Lett.*, 2015, **6**, 4653–4672.
- 69 D. I. Iermakova, R. Dugas, M. R. Palacín and A. Ponrouch, *J. Electrochem. Soc.*, 2015, **162**, A7060–A7066.
- 70 Y. Lee, J. Lee, J. Lee, K. Kim, A. Cha, S. Kang, T. Wi, S. J. Kang, H. W. Lee and N. S. Choi, *ACS Appl. Mater. Interfaces*, 2018, **10**, 15270–15280.
- 71 R. Dugas, A. Ponrouch, G. Gachot, R. David, M. R. Palacin and J. M. Tarascon, *J. Electrochem. Soc.*, 2016, **163**, A2333–A2339.
- 72 Y. Z. Qiuwei Shi, M. Wu, H. Wang and H. Wang, *Angew. Chem.*, 2018, **57**, 9069–9072.
- 73 R. Cao, K. Mishra, X. Li, J. Qian, M. H. Engelhard, M. E. Bowden, K. S. Han, K. T. Mueller, W. A. Henderson and J.-G. Zhang, *Nano Energy*, 2016, **30**, 825–830.
- 74 A. Basile, F. Makhlooghiazad, R. Yunis, D. R. MacFarlane, M. Forsyth and P. C. Howlett, *ChemElectroChem*, 2017, **4**, 986–991.
- 75 J. Lee, Y. Lee, J. Lee, S. M. Lee, J. H. Choi, H. Kim, M. S. Kwon, K. Kang, K. T. Lee and N. S. Choi, *ACS Appl. Mater. Interfaces*, 2017, **9**, 3723–3732.
- 76 J. Zheng, S. Chen, W. Zhao, J. Song, M. H. Engelhard and J.-G. Zhang, *ACS Energy Lett.*, 2018, **3**, 315–321.
- 77 Z. W. Seh, J. Sun, Y. Sun and Y. Cui, *ACS Cent. Sci.*, 2015, **1**, 449–455.
- 78 J. Song, G. Jeong, A. J. Lee, J. H. Park, H. Kim and Y. J. Kim, *ACS Appl. Mater. Interfaces*, 2015, **7**, 27206–27214.
- 79 D. Ruiz-Martínez, A. Kovacs and R. Gómez, *Energy Environ. Sci.*, 2017, **10**, 1936–1941.

- 80 H. Tian, Z. W. Seh, K. Yan, Z. Fu, P. Tang, Y. Lu, R. Zhang, D. Legut, Y. Cui and Q. Zhang, *Adv. Energy Mater.*, 2017, **13**, 1602528.
- 81 D. H. Snyder, V. I. Hegde and C. Wolverton, *J. Electrochem. Soc.*, 2017, **164**, A3582–A3589.
- 82 S. M. George, *Chem. Rev.*, 2010, **110**, 111–131.
- 83 C. Marichy, M. Bechelany and N. Pinna, *Adv. Mater.*, 2012, **24**, 1017–1032.
- 84 X. Meng, X. Q. Yang and X. Sun, *Adv. Mater.*, 2012, **24**, 3589–3615.
- 85 B. Ahmed, C. Xia and H. N. Alshareef, *Nano Today*, 2016, **11**, 250–271.
- 86 J. Liu and X. Sun, *Nanotechnology*, 2015, **26**, 024001.
- 87 D. Wang, J. Yang, J. Liu, X. Li, R. Li, M. Cai, T.-K. Sham and X. Sun, *J. Mater. Chem. A*, 2014, **2**, 2306.
- 88 X. Li, J. Liu, M. N. Banis, A. Lushington, R. Li, M. Cai and X. Sun, *Energy Environ. Sci.*, 2014, **7**, 768–778.
- 89 C.-F. L. Alexander, C. Kozen, A. J. Pearse, M. A. Schroeder, X. Han, L. Hu, S.-B. Lee, G. W. Rubloff and M. Noked, *ACS Nano*, 2015, **9**, 5884–5892.
- 90 E. Kazyak, K. N. Wood and N. P. Dasgupta, *Chem. Mater.*, 2015, **27**, 6457–6462.
- 91 W. Luo, C.-F. Lin, O. Zhao, M. Noked, Y. Zhang, G. W. Rubloff and L. Hu, *Adv. Energy Mater.*, 2017, **7**, 1601526.
- 92 Y. Zhao, L. V. Goncharova, A. Lushington, Q. Sun, H. Yadegari, B. Wang, W. Xiao, R. Li and X. Sun, *Adv. Mater.*, 2017, **29**, 1606663.
- 93 Y. Zhao and X. Sun, *ACS Energy Lett.*, 2018, **3**, 899–914.
- 94 X. Li, A. Lushington, J. Liu, R. Li and X. Sun, *Chem. Commun.*, 2014, **50**, 9757–9760.
- 95 D. M. Piper, J. J. Travis, M. Young, S. B. Son, S. C. Kim, K. H. Oh, S. M. George, C. Ban and S. H. Lee, *Adv. Mater.*, 2014, **26**, 1596–1601.
- 96 X. Li, A. Lushington, Q. Sun, W. Xiao, J. Liu, B. Wang, Y. Ye, K. Nie, Y. Hu, Q. Xiao, R. Li, J. Guo, T. K. Sham and X. Sun, *Nano Lett.*, 2016, **16**, 3545–3549.
- 97 L. Chen, Z. Huang, R. Shahbazian-Yassar, J. A. Libera, K. C. Klavetter, K. R. Zavadil and J. W. Elam, *ACS Appl. Mater. Interfaces*, 2018, **10**, 7043–7051.
- 98 Y. Zhao, L. V. Goncharova, Q. Zhang, P. Kaghazchi, Q. Sun, A. Lushington, B. Wang, R. Li and X. Sun, *Nano Lett.*, 2017, **17**, 5653–5659.
- 99 S. Choudhury, S. Wei, Y. Ozhables, D. Gunceler, M. J. Zachman, Z. Tu, J. H. Shin, P. Nath, A. Agrawal, L. F. Kourkoutis, T. A. Arias and L. A. Archer, *Nat. Commun.*, 2017, **8**, 898.
- 100 S. Wei, S. Choudhury, J. Xu, P. Nath, Z. Tu and L. A. Archer, *Adv. Mater.*, 2017, **29**, 1605512.
- 101 Y. J. Kim, H. Lee, H. Noh, J. Lee, S. Kim, M. H. Ryou, Y. M. Lee and H. T. Kim, *ACS Appl. Mater. Interfaces*, 2017, **9**, 6000–6006.
- 102 H. Wang, C. Wang, E. Matios and W. Li, *Nano Lett.*, 2017, **17**, 6808–6815.
- 103 P. Li, T. Xu, P. Ding, J. Deng, C. Zha, Y. Wu, Y. Wang and Y. Li, *Energy Storage Mater.*, 2018, **15**, 8–13.
- 104 C. Yang, K. Fu, Y. Zhang, E. Hitz and L. Hu, *Adv. Mater.*, 2017, **29**, 1701169.
- 105 A. P. Cohn, N. Muralidharan, R. Carter, K. Share and C. L. Pint, *Nano Lett.*, 2017, **17**, 1296–1301.
- 106 S. Liu, S. Tang, X. Zhang, A. Wang, Q. H. Yang and J. Luo, *Nano Lett.*, 2017, **17**, 5862–5868.
- 107 Y. Lu, Q. Zhang, M. Han and J. Chen, *Chem. Commun.*, 2017, **53**, 12910–12913.
- 108 Y. Xu, A. S. Menon, P. P. R. M. L. Harks, D. C. Hermes, L. A. Haverkate, S. Unnikrishnan and F. M. Mulder, *Energy Storage Mater.*, 2018, **12**, 69–78.
- 109 H. J. Yoon, N. R. Kim, H.-J. Jin and Y. S. Yun, *Adv. Energy Mater.*, 2018, **8**, 1701261.
- 110 Q. Zhang, Y. Lu, M. Zhou, J. Liang, Z. Tao and J. Chen, *Inorg. Chem. Front.*, 2018, **5**, 864–869.
- 111 S. Tang, Z. Qiu, X.-Y. Wang, Y. Gu, X.-G. Zhang, W.-W. Wang, J.-W. Yan, M.-S. Zheng, Q.-F. Dong and B.-W. Mao, *Nano Energy*, 2018, **48**, 101–106.
- 112 X. H. Aoxuan Wang, H. Tang, C. Zhang, S. Liu, Y.-W. Yang, Q.-H. Yang and J. Luo, *Angew. Chem.*, 2017, **129**, 12083–12088.
- 113 W. Luo, Y. Zhang, S. Xu, J. Dai, E. Hitz, Y. Li, C. Yang, C. Chen, B. Liu and L. Hu, *Nano Lett.*, 2017, **17**, 3792–3797.
- 114 Y. Zhao, X. Yang, L. Y. Kuo, P. Kaghazchi, Q. Sun, J. Liang, B. Wang, A. Lushington, R. Li, H. Zhang and X. Sun, *Small*, 2018, **14**, 1703717.
- 115 P. Hartmann, C. L. Bender, M. Vracar, A. K. Durr, A. Garsuch, J. Janek and P. Adelhelm, *Nat. Mater.*, 2013, **12**, 228–232.
- 116 J. Kim, H. Park, B. Lee, W. M. Seong, H. D. Lim, Y. Bae, H. Kim, W. K. Kim, K. H. Ryu and K. Kang, *Nat. Commun.*, 2016, **7**, 10670.
- 117 C. L. B. Lukas Medenbach, R. Haas, B. Mogwitz, C. Pompe, P. Adelhelm, D. Schröder and J. Janek, *Energy Technol.*, 2017, **5**, 2265–2274.
- 118 X. Bi, X. Ren, Z. Huang, M. Yu, E. Kreidler and Y. Wu, *Chem. Commun.*, 2015, **51**, 7665–7668.
- 119 J.-L. Ma, Y.-B. Yin, T. Liu, X.-B. Zhang, J.-M. Yan and Q. Jiang, *Adv. Funct. Mater.*, 2018, **28**, 1703931.
- 120 H. Yang, J. Sun, H. Wang, J. Liang and H. Li, *Chem. Commun.*, 2018, **54**, 4057–4060.
- 121 L. Lutz, D. Alves Dalla Corte, M. Tang, E. Salager, M. Deschamps, A. Grimaud, L. Johnson, P. G. Bruce and J.-M. Tarascon, *Chem. Mater.*, 2017, **29**, 6066–6075.
- 122 S. Wu, Y. Qiao, K. Jiang, Y. He, S. Guo and H. Zhou, *Adv. Funct. Mater.*, 2018, **28**, 1706374.
- 123 Z. L. Xiaofei Hu, Y. Zhao, J. Sun, Q. Zhao, J. Wang, Z. Tao and J. Chen, *Sci. Adv.*, 2017, **3**, 1602396.
- 124 X. Yu and A. Manthiram, *J. Phys. Lett.*, 2014, **5**, 1943–1947.
- 125 X. Yu and A. Manthiram, *Adv. Energy Mater.*, 2015, **5**, 1500350.
- 126 X. Yu and A. Manthiram, *Chem. Mater.*, 2016, **28**, 896–905.
- 127 Z. Zhang, Q. Zhang, J. Shi, Y. S. Chu, X. Yu, K. Xu, M. Ge, H. Yan, W. Li, L. Gu, Y.-S. Hu, H. Li, X.-Q. Yang, L. Chen and X. Huang, *Adv. Energy Mater.*, 2017, **7**, 1601196.
- 128 L. Duchêne, R. S. Kühnel, E. Stilp, E. Cuervo Reyes, A. Remhof, H. Hagemann and C. Battaglia, *Energy Environ. Sci.*, 2017, **10**, 2609–2615.
- 129 S. X. Hongcai Gao, L. Xue and J. B. Goodenough, *Chem*, 2018, **4**, 833–844.

- 130 S. Wenzel, T. Leichtweiss, D. A. Weber, J. Sann, W. G. Zeier and J. Janek, *ACS Appl. Mater. Interfaces*, 2016, **8**, 28216–28224.
- 131 E. A. Wu, C. S. Kompella, Z. Zhu, J. Z. Lee, S. C. Lee, I. H. Chu, H. Nguyen, S. P. Ong, A. Banerjee and Y. S. Meng, *ACS Appl. Mater. Interfaces*, 2018, **10**, 10076–10086.
- 132 W. Zhou, Y. Li, S. Xin and J. B. Goodenough, *ACS Cent. Sci.*, 2017, **3**, 52–57.
- 133 H. Tang, Z. Deng, Z. Lin, Z. Wang, I.-H. Chu, C. Chen, Z. Zhu, C. Zheng and S. P. Ong, *Chem. Mater.*, 2017, **30**, 163–173.
- 134 G. T. Kim, G. B. Appetecchi, M. Montanino, F. Alessandrini and S. Passerini, *ECS Trans.*, 2010, **25**, 127–138.
- 135 B. D. Adams, J. Zheng, X. Ren, W. Xu and J.-G. Zhang, *Adv. Energy Mater.*, 2018, **8**, 1702097.
- 136 M. N. Banis, H. Yadegari, Q. Sun, T. Regier, T. Boyko, J. Zhou, Y. M. Yiu, R. Li, Y. Hu, T. K. Sham and X. Sun, *Energy Environ. Sci.*, 2018, DOI: 10.1039/c8ee00721g.
- 137 E. Peled, D. Golodnitsky, H. Mazor, M. Goor and S. Avshalomova, *J. Power Sources*, 2011, **196**, 6835–6840.